X-630-72-49

PREPRINT

NASA TM X- 65897

INTERSTELLAR FORMALDEHYDE AND SILICON MONOXIDE IN ULTRA-DENSE CLOUDS

MARC LESLIE KUTNER

JANUARY 1972

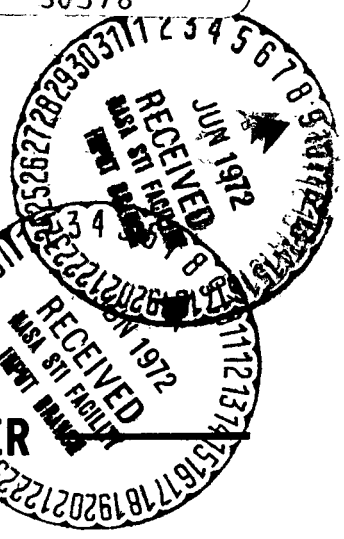

Goddard Institute for Space Studies
2880 Broadway, New York, N. Y.

GSFC — GODDARD SPACE FLIGHT CENTER
GREENBELT, MARYLAND

INTERSTELLAR FORMALDEHYDE AND SILICON MONOXIDE IN ULTRA-DENSE CLOUDS

Marc Leslie Kutner

Submitted in partial fulfillment
of the requirements for
The Degree of Doctor of Philosophy
in the Faculty of Pure Science
Columbia University
1972

ABSTRACT

Interstellar Formaldehyde and Silicon Monoxide in Ultra-Dense Clouds

Marc Leslie Kutner

The first part of this dissertation reports the discovery of the 140.8-GHz, 1_{11}-2_{12} and 150.5-GHz 1_{10}-2_{11} rotational transitions of ortho-formaldehyde and the 146.6-GHz 1_{01}-2_{02} transition of para-formaldehyde in the Orion Nebula. All lines were observed in emission. The 140.8-GHz line was mapped over a region $\sim 3' \times 5'$ in the direction of the Kleinmann-Low IR nebula. It is argued that the excitation is due to collisions with neutral particles, whose density is calculated to be $\sim 2 \times 10^5$ cm^{-3}, yielding a total mass of ~ 200 $M_\odot$ for the Kleinmann-Low nebula which is argued to be the central condensation of this cloud. The 140.8-GHz line was also detected in the direction of Sgr A, W3 (OH), W51, DR21 (OH) and NGC 2024.

The detection of weak 6-cm H_2CO absorption over much of the Orion Nebula is also reported. Because the line shows no correlation with the 6-cm continuum, it is attributed to "anomalous" absorption by H_2CO behind the H II continuum source. In the direction of the Kleinmann-Low IR nebula the line appears self-reversed, with an emission core of about 0.1 K that is identified with the 2-mm H_2CO emission in that direction. It is suggested that the

6-cm emission is a consequence of collisional quenching of the "anomalous" pumping mechanism.

The last section of this dissertation reports the detection of line emission attributed to the 130.246-GHz, $J = 3 \rightarrow 2$ rotational transition of silicon monoxide (SiO) in the direction of the source Sgr B2. The line was sought but not found in a number of other sources.

CONTENTS

CHAPTER I

INTRODUCTION

The study of interstellar molecules has experienced explosive growth in the past three years. Observations of the radio lines of interstellar molecules began with the discovery of OH (Weinreb et al. 1963). The first discoveries of polyatomic molecules - NH_3 and H_2O (Cheung et al. 1968; Cheung et al. 1969) - initiated the rapid development in this field. To date, over twenty molecules have been discovered in the interstellar medium, and it has now become clear that apart from questions of their formation, interstellar molecules are of considerable significance since their lines provide an important tool for the study of many classical astronomical problems (cf. Rank, Townes and Welch 1971).

One reason that no serious search was made for interstellar polyatomic molecules prior to 1968 was that observations implied an OH abundance down by a factor of 10^{-6} from that of hydrogen, possibly indicating a small probability of finding observable quantities of more complex molecules. Also there was a tendency to think in terms of "standard" interstellar H I clouds (cf. Spitzer 1968) whose density is ~ 10 cm^{-3} and where the visual extinction is less than one magnitude. In such clouds the lifetime against photodissociation of molecules is quite short — typically less than 100 years —

and it is noteworthy that polyatomic molecules have not yet been found in these regions. However, molecules have been found in regions of high density and presumably high opacity.

Current progress in this field largely results from the development of sensitive radio receivers, particularly in the 2 - 4 mm wavelength region. The millimeter region has also become particularly fruitful for the discovery of new molecules and for the study of regions of high density. The first interstellar molecular line discovered in this spectral range was the 2.6-mm transition of carbon monoxide (Wilson, Jefferts and Penzias 1970), which has been found to be so intense and widespread that its importance as a general tool for the study of H I regions and galactic structure may ultimately surpass that of the 21-cm line, its advantages being the ability to determine opacities from observations of isotopic species and the high angular resolution which can be obtained with moderate-sized antennae.

A molecule of considerable interest is formaldehyde (H_2CO), which surveys have shown to be very abundant in the Galaxy (Zuckerman et al. 1970; Whiteoak and Gardner 1970; Gardner and Whiteoak 1970; Scoville, Solomon and Thaddeus 1972). It has a number of observable transitions in both the centimeter and millimeter regions of the spectrum and exhibits a non-equilibrium pumping phenomenon, which, unlike the OH and H_2O masers,

appears over extended regions. The H_2CO rotational energy levels (Figure 1) are those of a nearly symmetric rotor with levels for $|K| > 0$ split into K-type doublets. Because of the spin of the hydrogen nuclei, formaldehyde is divided into ortho (K odd) and para (K even) species between which radiative and collisional transitions are so strongly forbidden that in interstellar space ortho and para formaldehyde can virtually be considered distinct molecules.

Formaldehyde was first discovered in the interstellar medium by the detection of the 4.83-GHz ($\sim$ 6 cm) 1_{11}-1_{10} transition in absorption against galactic continuum sources (Snyder et al. 1969). 6-cm absorption was also observed in dark clouds by Palmer et al. (1969) who concluded that the radiation being absorbed is the isotropic background radiation, indicating that the excitation temperature of the transition is less than 2.7 K. A survey of dark clouds (Dieter 1971) indicates that this phenomenon, termed "anomalous" absorption, is widespread.

Several mechanisms have been proposed to explain this cooling of the 6-cm transition. Townes and Cheung (1969) suggested that it results from collisions with neutral particles – H atoms, or more probably, H_2 molecules. However, Thaddeus (1972) has shown that quantum effects probably limit this mechanism to regions where the kinetic temperature is greater than 40 K, which observations indicate is well above that in the nebulae where "anomalous" absorption is

observed. Thaddeus and Solomon (1972) have shown that small deviations from a blackbody spectrum in the background radiation could cause the observed cooling. Litvak (1970) has proposed that the cooling is due to infrared line emission from formaldehyde in shock-heated layers deep within the cloud, and Oka (1970) has proposed that the cooling results from excitation at the time of H_2CO formation.

Besides the 6-cm line, a number of other formaldehyde transitions have been observed. The 14.49-GHz ($\sim$ 2 cm) 2_{12}-2_{11} transition has been detected by Evans, Cheung and Sloanaker (1970) and the 28.79-GHz ($\sim$1 cm) 3_{13}-3_{12} transition was found by Welch (1970). The 1_{11}-1_{10} transitions of the isotopic species $H_2{}^{13}C{}^{16}O$ at 4.59 GHz (Zuckerman et al. 1969) and $H_2{}^{12}C{}^{18}O$ at 4.39 GHz (Gardner, Ribes and Cooper 1971) have also been observed.

This dissertation is primarily devoted to new observations of interstellar formaldehyde. The first observations described here are of the three $J = 2 \rightarrow 1$ ($\lambda \approx 2$ mm) formaldehyde lines, one of which belongs to the para species. It was felt that the observation of these lines would shed light on the excitation of this molecule, and the observations were made possible by the development of the millimeter receiver mentioned above. In this study (see Chapter 3) the strongest 2-mm emission was found in the direction of the Kleinmann-Low infrared nebula in the Orion Nebula (Ori A), an H II region in which

the 6-cm line had not been detected by Zuckerman et al. (1970) in their initial survey.

These results led to the second set of observations reported here — a search for and study of 6-cm formaldehyde absorption in the direction of the Orion Nebula. These observations were undertaken since an analysis of the 2-mm observations indicated that a weak 6-cm line should be observable in this direction and, because of the high density deduced for this region, it appeared that its detection would yield information on the effects of collisions on the anomalous absorption process.

The final observations reported here are of a successful search for the $J = 3 \rightarrow 2$, 130-GHz transition of silicon monoxide (SiO). This discovery of SiO at 130 GHz, following an unsuccessful search by Dickinson and Gottlieb (1971) for the 87-GHz line, is an indication that the excitation in many ultra-dense regions is such that the higher frequency transitions are more easily detected.

CHAPTER II

APPARATUS AND OBSERVATIONAL PROCEDURE

Two radio telescopes of the National Radio Astronomy Observatory (NRAO) were used for the observations on which this dissertation is based. The 6-cm formaldehyde observations were made with the 140-foot antenna at Green Bank, West Virginia; the millimeter wavelength observations were made with the 36-foot antenna on Kitt Peak.

A. Millimeter Observations

The high sensitivity which has recently been achieved in millimeter receivers is due largely to the use of Schottky barrier diodes developed by C. A. Burrus of the Bell Telephone Laboratories. These were the mixer diodes used by Wilson, Jefferts and Penzias (1970) for the discovery of interstellar CO; essentially the same Bell Labs receiver was used for the observations reported here. Its double sideband noise temperature at 140 GHz was measured to be 800-1200 K, or a factor of more than 10 lower than had previously been obtainable.

The local oscillator klystron of the receiver was frequency-stabilized with the circuit shown schematically in Figure 2 (Weinreb 1970). The klystron was phase-locked to approximately the 75th harmonic of an oscillator ($\sim$ 2 GHz) which was in turn phase-

locked to a frequency synthesizer operating at about 100 MHz. The intermediate frequency (IF) of the receiver was 1390 MHz and this signal was amplified by a Micromega (~ 50 K) 21-cm parametric amplifier, so from the paramp on, the receiver is essentially a "standard" NRAO 21-cm receiver.

Two filter banks were available for use with this receiver. One, a 40-channel bank, used for most of the observations reported here, had filters 1.4 MHz wide (at 3dB points) and spaced 1 MHz apart. For higher resolution work a 50-channel filter bank, with 250-kHz channels spaced 250 kHz apart, was used. The details of the filter banks are given in NRAO reports (Thacker and Beale 1969; Ballister 1968).

All observations were made with frequency switching of the 2-mm local oscillator. Because of gain instabilities, it was necessary to make off-source observations to obtain reference spectra which were subtracted from the on-source spectra. In general, five minute on-source observations were alternated with off-source scans of equal duration. For the SiO observations, which were made somewhat later, the installation of a computer to control the telescope pointing allowed a modified procedure. Each scan consisted of ten cycles of 30 seconds on and 30 seconds off the source (equivalent to beam-switching once per minute). The question of calibration of this receiver is an important one and is discussed in Appendix A.

The 36-foot antenna is altitude-azimuth mounted and the feed horn was normally set with the E-plane parallel to the horizon, so that the E-plane rotated with respect to the source during observations. With this feed the half-power beam width (HPBW) at 2 mm was about 1' and the beam efficiency was 0.6.

B. 6-cm Observations

For observations on the 140-foot telescope the standard NRAO 6-cm receiver was used. With the cooled parametric amplifier the system noise temperature was between 85 and 100 K. The receiver was equipped with the NRAO 384-channel autocorrelator (Weinreb 1963; Shalloway et al. 1968) whose bandwidth may be varied up to 10 MHz. Most observations described here were made with spectral resolutions of 7.9 or 3.9 kHz.

Some observations were made without frequency or beam switching, an observing technique only feasible with very stable receivers. Before each series of scans on a source an off-source reference spectrum was taken. The final spectra were the differences between the on-source spectra and this reference spectrum. Other observations were made in the frequency switching mode for which off-source observations were unnecessary.

The 140-foot telescope is equatorially mounted and the observations were made with a linear feed whose E-plane was north-south. With this feed the HPBW at 6 cm was about 6' and the beam efficiency was 0.82.

C. Data Reduction

At both telescopes the spectra were displayed at the completion of each observation and were stored on magnetic tape for further processing. Preliminary processing of the 6-cm data was done with standard NRAO computer programs[1] which allowed for detection and deletion of bad records and produced a FORTRAN readable tape with the data for each observation stored as antenna temperature for each channel. For all data, final reduction was done on the IBM 360/95 computer at the Goddard Institute for Space Studies. When several observations were made at a given location they were generally synthesized to improve signal-to-noise. The spectra were Gaussian filtered where appropriate, and Kitt Peak observations were corrected for atmospheric attenuation (see Appendix B).

---

[1] Programs AC4141A, AC4142A, TPOWER1 and TPOWER2 (cf. Farris et al. 1968).

CHAPTER III
OBSERVATIONAL RESULTS

A. 2-mm Formaldehyde Observations[1]

In October, 1970 the 140.8-GHz 1_{11}-2_{12} formaldehyde transition was detected in emission around the direction of the Kleinmann-Low (1967) infrared nebula in the Orion Nebula (Ori A), an HII region where the 6-cm line was absent (Zuckerman et al. 1970). At that time only upper limits were obtained for this transition in a number of Galactic HII regions and in two dark nebulae where 6-cm H_2CO absorption had previously been observed (Zuckerman et al. 1970; Palmer et al. 1969).

This work was continued with a more sensitive receiver in February, 1971. The 1_{10}-2_{11} and 1_{01}-2_{02} transitions were detected in Ori A, also in emission, at 150.5 and 145.6 GHz, the latter transition belonging to the previously undetected para species of the molecule. An upper limit was also obtained in Ori A for the 1_{10}-2_{11} transition of the isotopic species $H_2{}^{13}CO$, which falls at 146.6 GHz. During this run, the 140.8-GHz line was also detected in three other sources: Sgr A, W51 and W3 (OH). In December, 1971 this line was detected in Ori B (NGC 2024) and DR 21 (OH) and an upper limit was obtained in Ori A for the 137.4-GHz 1_{11}-2_{12} transition of $H_2{}^{13}CO$.

---

[1] These observations were made in collaboration with P. Thaddeus, K. B. Jefferts, A. A. Penzias and R. W. Wilson and have, at least in part, been described in Kutner et al. (1971) and Thaddeus et al. (1971).

A1. Observations in the Orion Nebula

The results of the 2-mm formaldehyde observations in the direction of the Kleinmann-Low nebula are summarized in Table 2 and Figures 4, 5, 6, 7 and 8. Table 2 gives the location, antenna temperature and radial velocity of the observed lines. Radial velocities are based on the laboratory rest frequencies given in Table 1. The antenna temperatures in Table 2 have been corrected for atmospheric attenuation by the method of Appendix B. After correcting for beam efficiency and for line broadening by the receiver filters (Appendix C), the line brightness temperatures are about 2.2 times the antenna temperatures. Measurements of the antenna temperatures for a given line at separate locations are relatively accurate to 5-10%, but because of the calibration uncertainty described in Appendix A, the absolute scale of antenna temperatures and the relative values for different lines are uncertain by 25%.

Figure 3 shows the spectra of the three $J = 2 \rightarrow 1$ H_2CO lines at the location marked "C" in Figure 6, a point which lies near the peak of 140.8-GHz emission. The lines shown agree in velocity and width with those of CO (Wilson et al. 1970), CS (Penzias et al. 1971) and CN (Jefferts et al. 1971) in this direction. Upper limits were obtained for the 146.6-GHz transition of $H_2{}^{13}CO$ at this location, and for the 137.4-GHz $H_2{}^{13}CO$ transition at position B (see Table 2).

A crude map of the extent of the 140.8-GHz emission around the direction of the Kleinmann-Low nebula, based on the October, 1970 data, is shown in Figure 4. A better map of the same region, based on the February, 1971 data is shown in Figure 5; the observations were generally spaced one-half a beamwidth apart in the center of the source and a full beamwidth apart on its fringes. The velocity over the field is measured to be constant to within the velocity resolution of 2.2 km/sec. Figure 6 shows a contour map of the 140.8-GHz emission, made from the observations in Figure 5. The emission is sharply peaked in the direction of the IR continuum peak, the IR star (Becklin and Neugebauer 1967) and the OH maser (Raimond and Eliasson 1967) about 1' from the Trapezium. The CO and CS emission in Orion also peak in this direction, with the CS having a slightly greater extent than the H_2CO, and the CO extending in right ascension and declination considerably farther than either (Penzias et al. 1971; Wilson, Jefferts and Penzias 1970). In Figure 12, the 140.8-GHz formaldehyde contour map is superimposed on a photograph of the Orion Nebula, and it is apparent that only a small part of the nebula has been surveyed at 140.8 GHz.

Figures 7 and 8 show the results of limited mapping of the 150.5- and 145.6-GHz lines.

A.2 2-mm Observations in Other Sources

Following the initial unsuccessful search for the 140.8-GHz formaldehyde line in other sources (see Table 3) this line was found

in emission in the sources W 3(OH), W 51, Sgr A (NH_3A), Ori B (NGC2024) and DR21(OH). These observations are summarized in Table 4 and Figures 9, 10, and 11. Table 4 gives the line antenna temperature, velocity and doppler width at each position at which the line was observed. Figure 9 shows the strongest line in three of these sources superimposed on the 4.83-GHz absorption spectra of Zuckerman et al.(1970) and the HCN 88.6-GHz emission spectra of Snyder and Buhl (1971). Figures 10 and 11 show the results of limited mapping of the 140.8-GHz line in W 51 and W 3(OH) (as tabulated in Table 4).

In Sgr A the detected 0.8 K line is located 2.5' south and slightly to the east of the location where an upper limit of 0.7 K had previously been obtained (Table 2) perhaps indicating that the Sgr A source is small. In W 51 the line is found near the 2-cm continuum peak (Schraml and Mezger 1969). Also, marginal evidence for a line in W 51 was found about 1^m (i.e., 15 beamwidths) east of this location at $\alpha(1950) = 19^h22^m28^s$, $\delta(1950) = 14° 24' 16''$ and at $\alpha = 19^h22^m28^s$, $\delta = 14° 25' 16''$. The suspected feature has an antenna temperature of about 1 K and a radial velocity of +65 km/sec approximately equal to that of the strong 4.83-GHz absorption line, but it appears to be wider than the 4.83-GHz line.

In W 3(OH), W 51 and Sgr A the velocity and width of the 140-GHz emission profile agree with that of the 88.6-GHz HCN line (Snyder and Buhl 1971) and with that of the 147-GHz CS line in W 51 and DR21(OH) (Penzias et al. 1971). Distinct differences, notably in Sgr A and W 51, exist between the velocities of the 140-GHz and 4.83-GHz formaldehyde lines. This may give indications as to the inhomogeneity of these regions and may imply that the conditions necessary to excite these millimeter transitions exist in only a small portion of the molecular clouds in these sources.

In W 51, W 3(OH) and DR21(OH), the 140-GHz line, as in the Orion Nebula, appears to peak on, or at least very near, point sources of both OH (Raimond and Eliasson 1969; Palmer and Zuckerman 1967) and H_2O emission (Knowles et al. 1969). From preliminary mapping (Figures 10 and 11) it appears that the 140.8-GHz sources, while small, are distinctly extended.

B. 6-cm Formaldehyde Observations in the Orion Nebula

The discovery of the 2-mm H_2CO emission in the Kleinmann-Low nebula motivated a search in that direction for the 6-cm H_2CO line. The observations were made in April, 1971 with the 140-foot telescope.[1] The observations are summarized in Table 5 and Figures 12 and 13. Table 5 gives the peak line brightness temperature at each position, the line velocity and full width at half intensity and the continuum brightness temperature, either from Mezger and Henderson's (1967) 6-cm map of Ori A or extrapolated from 8-GHz continuum temperatures of Gordon and Meeks (1968; Meeks 1971).

Figure 12 is a photograph of the Orion Nebula showing the locations observed at 6 cm. Figure 13 shows the 6-cm spectra at the numbered positions; 6-cm absorption is found over much of the Orion Nebula at an intensity of 0.1 to 0.5 K. Position 17, where the line has a self-reversed appearance, (which will be discussed below), centers on the Kleinmann-Low IR nebula and the small source of 2-mm H_2CO emission; it also contains the 6-cm continuum peak (Mezger and Henderson 1967). The continuum radiation falls off rapidly on the scale of Figure 12 and has not been detected below position 12.

---

[1] These observations were made with P. Thaddeus and the results have been published, in part, in Kutner and Thaddeus (1971).

C. Observations of Interstellar Silicon Monoxide

The observations in this section were made in April, 1971 using the 36-foot antenna.[1]

Line emission from the Galactic radio source Sgr B2 has been observed at a frequency of 130.246 GHz (with respect to the local standard of rest), which is attributed to the $J = 3 \rightarrow 2$ rotational transition of the silicon monoxide molecule. The signal obtained in the direction of the OH point emission sources in Sgr B2 (Raimond and Eliasson 1969) is shown in Figure 15. A summary of the data here and at one other location where observations were obtained in Sgr B2 is given in Table 6. After correction for the line broadening by the filters, the atmospheric attenuation and the beam efficiency, the line radiation temperatures are about two times the antenna temperatures.

This line was sought in a number of other sources, but it was not found. The negative results are summarized in Table 7.

---

[1] These observations were made in collaboration with P. Thaddeus, K. B. Jefferts, A. A. Penzias and R. W. Wilson, and the results published, in part, in Wilson et al. 1971.

CHAPTER IV

DISCUSSION

From the observations reported in the previous chapter, it is possible to obtain a considerable amount of information about the molecular excitation and the physical conditions responsible for it. In the first part of this section, an analysis of the formaldehyde observations in the Orion Nebula is presented. Excitation of the 2-mm H_2CO lines is discussed and an estimate of the neutral particle density in the Orion molecular cloud is obtained. Also, from the Orion Nebula observations, conclusions are drawn about the relationship of the molecular cloud, the IR nebula and Becklin's IR star. An estimate is made of the H_2CO ortho-para ratio. Information on the anomalous pumping mechanism is provided by these 2-mm observations and by the 6-cm Ori A observations. The final section contains an analysis of the silicon monoxide observations.

Before proceeding to the discussion, it will be useful to outline certain basic definitions, relations and assumptions which will recur in the subsequent analysis.

Radio measurements are often given in terms of brightness temperature T_B or radiation temperature T_R, rather than the intensity of radiation I_ν. I_ν is related to T_B by the Planck function

$$I_\nu = \frac{2h\nu^3}{c^2}\left(e^{h\nu/kT_B} - 1\right)^{-1} , \qquad (4.1a)$$

and to T_R by the Rayleigh-Jeans formula

$$T_R = \frac{c^2 I_\nu}{2\nu^2 k} . \qquad (4.1b)$$

Clearly, T_B and T_R are equal for $h\nu \ll kT_B$. For the observations reported here the receivers were always calibrated against sources for which it was assumed that the temperature was proportional to the radiation intensity, so the results are always in terms of radiation temperatures.

Consider now, two molecular levels 1 and 2 with energies $E_1 < E_2$, populations n_1 and n_2 and statistical weights g_1 and g_2. The excitation temperature, T_{21}, is defined by

$$\frac{n_2}{n_1} = \frac{g_2}{g_1} e^{-h\nu/kT_{21}} \qquad (4.2)$$

where $h\nu = E_2 - E_1$. Suppose now that the molecules in question lie in front of a continuum source of radiation temperature T_C, and are immersed in background radiation of temperature T_{BG}. The line radiation temperature, which is defined to be the

difference in radiation temperature between the line center and the continuum, is given by (cf. Kerr 1968)

$$T_R = (T_{21} - T_C - T_{BG})\,(1 - e^{-\tau_\nu}) \qquad (4.3)$$

where τ_ν is the optical depth at the line center. If $T_{21} > (T_C + T_{BG})$ the line is seen in emission; if $T_{21} < (T_C + T_{BG})$ it is in absorption. The observed antenna temperature T_A of the line will, in addition, depend on the antenna beam efficiency, η, and the size of the antenna beam with respect to the source. If the source fills the beam then

$$T_A = \eta T_B \qquad (4.4a)$$

and if it is much smaller then the beam

$$T_A = \frac{\Omega_S}{\Omega_M}\eta T_B \qquad (4.4b)$$

where Ω_M is the solid angle of the main antenna beam, and Ω_S is that subtended by the source.

For allowed electric dipole transitions, the optical depth in the line center τ_o is given by (cf. Kerr 1968)

$$\int_{\text{line}} \tau_\nu d\nu = \frac{8\pi^3\nu}{3hc}|\mu_{21}|^2\left(\frac{g_2}{g_1}N_1 - N_2\right) \qquad (4.5)$$

$$\approx \tau_o\,\Delta\nu$$

where N_1 and N_2 are the indicated column number densities, $|\mu_{21}|^2$ is the summed squared dipole matrix element for the transition, and $\Delta\nu$ is the full line width at half maximum. We are often interested in the case $h\nu \ll kT_{21}$, for which equations (4.2) and (4.5) give

$$\tau = \frac{8\pi^3\nu^2}{3ckT_{21}\Delta\nu} |\mu_{21}|^2 N_2 = \frac{8\pi^3\nu^2}{3ckT_{21}\Delta\nu} |\mu_{21}|^2 \frac{g_2}{g_1} N_1 \quad . \quad (4.6)$$

If $h\nu \ll kT_{21}$ and in addition, $\tau \ll 1$

$$T_R = (T_{21} - T_C - T_{BG})\,\tau = \frac{8\pi^3\nu^2 N_2}{3ck\Delta\nu} |\mu_{21}|^2 \left(1 - \frac{T_C + T_{BG}}{T_{21}}\right). \quad (4.7)$$

H_2CO is a nearly symmetric top, and the electric dipole matrix elements are given to sufficient accuracy by (cf. Thaddeus 1972)

$$|\mu_{K'J';KJ}|^2 = (2J+1)\begin{pmatrix} J' & 1 & J \\ -K' & 0 & K \end{pmatrix}^2 \mu^2 \quad (4.8)$$

where $\mu = 2.34 \times 10^{-18}$ esu is the H_2CO permanent electric dipole moment (cf. Townes and Schawlow 1955), the bracket denotes the Wigner 3j symbol and the $'$ denotes the initial state. Spontaneous radiative decay will then occur at the rate

$$A_{K'J',KJ} = \frac{64\pi^4\nu^3\mu^2}{3hc^3} (2J+1) \begin{pmatrix} J' & 1 & J \\ -K' & 0 & K \end{pmatrix}^2 \quad . \quad (4.9)$$

The treatment used above for the determination of line strengths, though widely used in the analysis of radio observations, formally applies only in the optically thin case, in which the problems of line formation are straightforward. Using the numerical technique of Auer and Mihalas (1969; 1970), White (1970) has considered the problem of non-LTE radiative transfer in the four lowest levels of ortho formaldehyde, taking into account the effects of finite optical depth. The problem considered was that of a cloud immersed in 2.7 K background radiation, with the formaldehyde collisionally excited by electrons and neutrals (taken to be H_2 molecules). For rates of H_2CO excitation by collisions with H_2 molecules, White used the results of Thaddeus (1972) who considered four excitation models: (1) S-wave scattering from only the formaldehyde H atoms in the sudden approximation, (2) S-wave scattering from all four formaldehyde atoms in the sudden approximation, (3) S-wave scattering from the H atoms without the use of the sudden approximation and (4) scattering from finite-sized H atoms in the sudden approximation. White used the rates from the first model since this showed the strongest collisional cooling of the 6-cm transition in the optically thin limit. However, in the optically thin case the behavior of the millimeter lines is not significantly model-dependent. Therefore, for this study it is assumed that White's results adequately describe the excitation of the millimeter lines.

White found that for neutral excitation the 2-mm transitions will remain in equilibrium with the background radiation until the densities become appreciable ($n_{H_2} \sim 10^4$ cm^{-3}), possibly explaining the negative results reported here for the 140.8-GHz line in a number of sources. He presented solutions for the line brightness temperatures as a function of neutral particle density for various values of the electron-to-hydrogen ratio and the formaldehyde column density.

In the following analysis of the 2-mm observations in the direction of the Kleinmann-Low nebula, White's results are used to obtain an estimate of neutral particle density from the observed formaldehyde column density. We first consider the location of the molecules relative to the Orion Nebula H II region.

A. Location of the Orion Molecular Cloud

With the discovery of an extended source of 2-mm H_2CO emission, the failure of Zuckerman et al. (1970) to detect 6-cm absorption in Ori A indicates that the H_2CO molecules are located behind the Trapezium and enveloping H II region. This idea is supported by the observations of the 6-cm line reported here in which the line strength shows an inverse correlation with the continuum intensity (see §F below).

Also, O. C. Wilson et al. (1959) suggest that the gas surrounding the Orion Nebula is expanding with a velocity of about 10 km/sec and Gordon and Meeks (1968) observe the velocity of the H94α line in the core of the H II region to be -3 km/sec (LSR). Therefore, the observed velocity of the molecular line ($\sim$8 km/sec) would place the molecules behind the H II region. There is strong additional evidence that the molecules are located behind the Orion Nebula. One of the molecules detected at millimeter wavelengths in this direction is CN (Jefferts, Penzias and Wilson 1970) which has also been observed in other interstellar clouds in optical absoption (cf. Adams 1949; Clauser 1969; Bortolot 1972). The column number density of CN molecules in the direction of Ori A has been estimated from the radio observations to be 1.1×10^{15} cm^{-2}. A very small fraction of these, perhaps as few as 5×10^{-3}, lying in front of θ^1C Ori, the brightest Trapezium star, would produce detectable optical absorption at 3874.6Å, yet neither this, nor any other molecular optical line, has been found there (Adams 1949).

Thus there can be little doubt that the Orion molecular cloud lies behind the H II region. Figures 12 and 13 indicate the extent of this cloud relative to the visible portion of the nebula.

B. Excitation of the Millimeter Lines

We now investigate the excitation mechanism responsible for 2-mm H_2CO emission. If the observed transitions are not saturated then the peak line brightness temperature of about 7 K is a lower limit to the excitation temperature T_{ex} of these transitions. To account for $T_{ex} \geq 7$ K requires that collisions, or photoexcitation of the optical or infrared transitions of H_2CO, occur at a rate comparable to or greater than the spontaneous decay rate of the upper (2_{12}) level; which by equation (4.9) is

$$A_{21} = 5.3 \times 10^{-5} \text{ sec}^{-1} \quad . \tag{4.10}$$

H_2CO readily photodissociates in the blue. For $2000\text{Å} < \lambda < 3600\text{Å}$, the quantum yield for photodissociation (molecules decomposed per photon absorbed) is greater than 0.9 (Stief 1971) and though one might conceive of some special mechanism which effectively cuts off radiation at wavelengths below 3600Å, it is probably reasonable to assume that the rate of photodissociation would be of the same order as the rate of photoexcitation. From the observed H_2CO column density (equation (4.20) below) this would imply a destruction rate

$$R_{diss} \sim 1.5 \times 10^{10} \text{ molecules/cm}^2\text{/sec} \quad . \tag{4.11a}$$

An upper limit on the production rate can be approximated by

assuming that for every CO molecule which hits a grain, an H_2 molecule also hits this grain, directly forming an H_2CO molecule which then evaporates. The production rate is then

$$R_{prod} = \pi r_g^2 v n_g N_{CO} \quad , \tag{4.11b}$$

where r_g is the grain radius taken to be 2×10^{-5} cm (cf. Gaustad 1963), v is the r.m.s. CO velocity at $T_{kin} = 60$ K, N_{CO} is the CO column density which may be as great as 10^{20} cm^{-2} (due to saturation the CO column density is uncertain; Wilson, Jefferts and Penzias 1970; Penzias, Jefferts and Wilson 1971) and n_g is the density of grains. If photoexcitation is responsible for the 2-mm emission then equation (4.21) below becomes an upper limit to the hydrogen density, which from van de Hulst's (1949) gas-to-dust ratio implies $n_g < 6 \times 10^{-8}$ cm^{-3}. This yields a production rate

$$R_{prod} \sim 10^7 \text{ molecules/cm}^2\text{/sec} \tag{4.11c}$$

which is a factor of roughly 1000 below the necessary production rate given in equation (4.11a). For this reason, this process of optical excitation is rejected.

Vibrational photoexcitation does not of course suffer from this

objection, but it is unlikely to occur at the required rate, as the following argument shows.

The two low-frequency bending vibrations ν_5 and ν_6 of H_2CO fall respectively at 1280 and 1167 cm^{-1} (Herzberg 1945, p. 300). In this frequency range it is known from the 11.6μ observations of Ney and Allen (1969) that the brightness temperature T_B of the nebula in the vicinity of the IR star is about 100 K; an upper limit to the rate of vibrational photoexcitation is then obtained if it is assumed that the molecules are not simply in the vicinity of, but are surrounded by the nebula, and are thus immersed in blackbody radiation at this temperature. Consider for simplicity only excitation of the ν_6 transition. Matrix elements for infrared vibrational transitions are difficult to calculate, and few have been measured. To make an estimate of $|\mu|^2$ consider first a diatomic molecule with bond length r_o (so the rotation constant $B = h/8\pi Mr_o^2$, where M is the reduced mass of the two atoms). Then the summed squared matrix element for the stretching vibration is given by

$$|\mu|^2 = \langle \frac{\partial \mu}{\partial r}(r - r_o)\rangle^2 \sim \frac{\mu^2}{r_o^2}\langle r - r_o\rangle^2 \quad . \qquad (4.12a)$$

For an harmonic oscillator at frequency ν, $\langle r - r_o\rangle^2 = h/2\pi^2 M\nu$, so

$$|\mu|^2 \sim 4\mu^2 B/\nu \quad . \qquad (4.12b)$$

Thus for the H_2CO ν_6 transition, we take as an upper limit to $|\mu|^2$, $\mu^2 A_o/\nu_6$, where A_o is the largest rotation constant of H_2CO (A_o = 2.82×10^{11} sec^{-1}). This upper limit corresponds to an f-value (oscillator strength) of 2.4×10^{-5}; the table below (taken from Penner 1959) shows that this is probably a conservative upper limit.

Molecule	$\nu(cm^{-1})$	f-value
CO	2,143	1.09×10^{-5}
	4,260	7.5×10^{-8}
OH	3,568	4.0×10^{-6}
	6,971	1.7×10^{-7}
H_2O	1,595	1.3×10^{-5}
	3,755	4.5×10^{-6}
	5,331	1.3×10^{-6}
	7,250	8.0×10^{-7}
	8,807	2.5×10^{-8}

Blackbody photoexcitation will then proceed at a rate

$$R_{ir} \leq \frac{64\pi^4 \nu_6^2 \mu^2 A_o}{3hc^3} e^{-h\nu_6/kT_B} \approx 1 \times 10^{-6} \text{ sec}^{-1} \qquad (4.13)$$

which is small with respect to A_{21} as given by equation (4.10). It is thus concluded that neither optical nor IR photons are likely to excite the H_2CO molecules at the required rate, leaving collisions as the probable mechanism.

In calculating collisional excitation rates it is assumed that H_2CO and CO, because of their similar line profiles, are coextensive over the central region of the molecular cloud where the 140.8-GHz line is observed, and that since the 115-GHz CO line is undoubtedly saturated (Penzias, Jefferts and Wilson 1971), its approximately 60 K brightness temperature is a good measure of the kinetic temperature T_{kin}.

We first consider excitation by collisions with charged particles. Excitation of H_2CO by ions at this temperature is negligible compared to excitation by electrons. The collisional rate from the 1_{11} to the 2_{12} level for electron excitation is adequately described in the Born approximation at $T_{kin} \approx 60$ K (cf. Allison and Dalgarno 1971), and is given by (cf. Thaddeus 1972)

$$R_{12} = \frac{64 n_e}{5}\left(\frac{\pi \mu e}{h}\right)^2\left(\frac{\pi m_e}{8kT_{kin}}\right)^{\frac{1}{2}}\left[\ell n\left(\frac{4kT_{kin}}{h\nu}\right) - 0.577\right] = 2.2 \times 10^{-6} n_e \cdot \tag{4.14}$$

If transitions to other levels are neglected, in statistical equilibrium $R_{12} = A_{21}(g_2/g_1)\,[\exp(h\nu/kT_{ex}) - 1\,]^{-1}$ for which $T_{ex} \geq 7$ K yields $R_{12} \geq 1.7\, A_{21} = 9.5 \times 10^{-5}$ sec^{-1}. So from equation (4.14) we see that an electron density of

$$n_e \geq 45 \text{ cm}^{-3} \tag{4.15}$$

is required to produce the observed excitation.

If excitation by electrons is the dominant mechanism then equation (4.21) becomes an upper limit for the neutral particle density, and by equation (4.15) this would imply a fractional ionization, n_e/n_{H_2}, in excess of 2×10^{-4}. The high observed infrared opacity of this region implies a density of dust great enough such that it is improbable that enough starlight will penetrate to produce this ionization. The presence of molecules promotes rapid dissociative recombination of those electrons which might be produced by X-rays or cosmic rays. There is also observational evidence that the excitation of the millimeter lines is primarily by collisions with neutrals rather than electrons. For electrons, the excitation rates, as in equation (4.14), are proportional to μ^2, as are the rates of spontaneous decay, so one would expect that for molecules with significantly different dipole moments, transitions in this frequency range would have essentially the same excitation temperature. Neutral excitation rates do not depend strongly on μ and molecules with higher dipole moments would be expected to have lower excitation temperatures due to the faster spontaneous decay rates. Therefore, the low observed excitation in this region of HCN (Snyder and Buhl 1971) and CS (Penzias et al. 1971) — molecules whose dipole moments are large — with respect to CO (Wilson et al. 1970) — whose moment is small — indicates that impact by neutral particles, not electrons, is responsible for the 2-mm H_2CO excitation.

We can now estimate the density of neutral particles required to produce the observed emission, by first considering the observed absence of 2-mm emission by $H_2{}^{13}CO$. It is reasonable to assume that the $^{12}C/^{13}C$ abundance ratio in the Orion Nebula has essentially the terrestrial value 89. Bortolot and Thaddeus (1969) and Smith and Stecher (1971) from optical spectroscopy have found comparable values of this ratio from, respectively, CH^+ and CO molecules in front of the star ζ Oph; Vanden Bout and Thaddeus (1971) find that the ratio is greater than 31 for CH^+ in front of 20 Tauri. The terrestrial ratio is also compatible with the results obtained by Zuckerman et al. (1969) in a 6-cm search for $H_2{}^{13}CO$, except possibly in the region of the Galactic center.

Using this ratio we first find an upper limit to the optical depth on the 146.6-GHz $H_2{}^{13}CO$ line in Ori A by assuming that this and the 150.5-GHz transition of $H_2{}^{12}CO$ have the same excitation temperature. Then by equations (4.3) and (4.5), we have

$$\frac{T_A{}^{13}}{T_A{}^{12}} = \frac{(1 - e^{-\tau})}{(1 - e^{-\tau/89})} . \qquad (4.16)$$

where τ and $\tau/89$ are the optical depths of the 150.5-and 146.6-GHz lines. Taking $T_A{}^{12}$ and the upper limit to $T_A{}^{13}$ from position "C" in Table 2 yields

$$\tau < 6$$
$$\tau / 89 < 0.07 \quad . \tag{4.17}$$

It is therefore clear that the 146.6-GHz line must be optically thin. Then equations (4.7) and (4.8) with $T_{21} >> (T_C + T_{BG})$ give

$$T_B = 2.2\, T_A = \frac{c^2 f N A_{21} h}{8\pi \nu \Delta\nu k} \tag{4.18}$$

where f is the fraction of ortho molecules in the 2_{11} level.

An upper limit to the column density of normal ortho molecules is obtained by applying equation (4.14) to the undetected 2-mm $H_2{}^{13}CO$ line ($T_A < 0.2$ K), setting $N = N_{ORTHO}/89$, and assigning as a lower limit to f the value of 4.4% obtained when all ortho levels are in equilibrium at 60 K, the cloud kinetic temperature adopted above. Similarly, a lower limit to N_{ORTHO}, valid even if the line is optically thick, is obtained by applying equation (4.18) to either the 140- or 150-GHz transition of normal formaldehyde, and assigning as a reasonable upper limit to f the value 5/16 obtained if only the J=1 and 2 levels are populated, each in proportion to its statistical weight. The limits so obtained are

$$6 \times 10^{13} \leq N_{ORTHO} \leq 1.8 \times 10^{15} \text{ cm}^{-2} \quad . \tag{4.19}$$

Thus a reasonable value to adopt for N_{ORTHO} in Ori A is

$$N_{ORTHO} \sim 3 \times 10^{14} \text{ cm}^{-2} \quad , \tag{4.20}$$

which, according to equation (4.19), must be considered uncertain by at least half an order of magnitude.

Though Thaddeus' (1972) excitation rates were computed for excitation by H_2 molecules, the results do not change significantly if the neutrals are taken to be H atoms, so the results below do not depend strongly on whether the neutrals are taken to be H or H_2. Theoretical studies (cf. Hollenbach, Werner and Salpeter 1970) indicate that in regions with extinctions greater than a few magnitudes, H_2 molecules should predominate over H atoms. This is consistent with the results of Carruthers (1970) who found the concentration of molecular and atomic hydrogen approximately equal in front of ξ Persei, where the optical extinction is about 1 mag, and did not find H_2 in front of ϵ Persei, where the extinction is lower. Therefore, the neutrals in the Kleinmann-Low nebula are taken to be mainly H_2.

We then find from White's (1970) theoretical investigation of the formation of interstellar H_2CO lines that if N_{ORTHO} is given by equation (4.20), a density of hydrogen molecules equal to

$$n_{H_2} \sim 2 \times 10^5 \text{ cm}^{-3} \qquad (4.21)$$

is required to produce a $\sim$7 K emission line at 140 or 150 GHz. At the distance of the Orion Nebula, 3' corresponds to 1.2×10^{18} cm; the assumption that the cloud is of equal extent in the line of sight then implies

$$N_{H_2} \sim 2 \times 10^{23} \text{ cm}^{-2} \quad , \tag{4.22}$$

and a formaldehyde-to-molecular-hydrogen ratio of

$$N_{H_2CO}/N_{H_2} \sim 2 \times 10^{-9} \tag{4.23}$$

which is in quite good agreement with the results obtained from 4.83-GHz absorption in a dark cloud by Kutner (1972) and in a number of sources (Zuckerman et al. 1970). The overall mass of the cloud derived from these figures is then

$$M \sim 230 \, M_{\odot} \tag{4.24}$$

which, again, is uncertain to at least half an order of magnitude.

One important point must be emphasized with regard to the millimeter observations. It has been shown that H_2CO emission in Ori A probably results from collisional impact, and that the total density required to excite the line is high — so high in fact that star formation must be taking place at a rapid rate. Since this conclusion may hold for other sources, and also for the recently discovered lines of HCN, CN, and CS (whose rotational radiative transition rates are comparable to that of H_2CO), it carries the important implication that millimeter wavelength molecular emission lines are generally signs of ultra-dense regions, and for

the first time provide spectroscopic tools for the study of the collapse of interstellar clouds and for the formation of stars.

It is also a striking fact that four out of the six sources of 140.8-GHz emission, all apparently small extended sources, peak on or very near point sources of OH and H_2O emission. This correlation might conceivably be an effect of observational selection, but it is more likely an indication that within the center of the observed clouds the density is so high that stars or protostars have already formed. It is noteworthy that in Ori A, at least, one reaches the same conclusion by considering the relation of the molecular cloud to the IR Nebula, as we shall now see.

C. Relationship of the Molecular Cloud to the IR Nebula

It is evident from the foregoing density estimates that the molecular cloud in Ori A must be extremely opaque. The usual interstellar extinction ratio, 1×10^{21} H_2 molecules per magnitude (cf. Spitzer 1968), implies by equation (4.22) a visual extinction,

$$E_v \sim 200 \text{ mag} \quad , \tag{4.25}$$

so large that even the infrared opacity of the cloud is appreciable. Taking the gas-to-dust ratio of van de Hulst (1949), equation (4.22) implies a column density of grains,

$$N_g \sim 6 \times 10^{10} \text{ cm}^{-2} \quad . \tag{4.26}$$

Krishna Swamy (1971) finds that the refractive index of the grains in the Kleinmann-Low nebula is similar to that of ice or silicate. At $\lambda = 10\mu$, Gaustad (1963) finds that the absorptive cross section for ice is $3.44 \times 10^{-11} \text{cm}^2$ and Knacke's (1968) results for silicates yield an absorptive cross section of $\approx 1 \times 10^{-10} \text{cm}^2$ at this wavelength. Using these cross sections with the grain column density given in equation (4.26) implies opacities, $\tau = N\sigma$, at 10μ of

$$\begin{aligned} \tau_{ice} &\approx 2.5 \\ \tau_{silicate} &\approx 6 \quad . \end{aligned} \tag{4.27}$$

Thus, if an infrared nebula had not already been found in this direction one would be led to hypothesize its existence. This means, as does the coincidence of the 140.8-GHz emission peak with that of the IR continuum (Figures 4 and 6), that the infrared nebula discovered by Kleinmann and Low (1967) is probably the central condensation of the molecular cloud, an idea supported by the agreement which exists between the above estimates of density and extinction and those derived by Kleinmann and Low and Hartmann (1967) from analysis of the IR data.

The equality of the peak brightness temperature of the saturated 115-GHz CO line (~60 K) and the peak brightness temperature of the IR Nebula (~77 K at 20 μ) is therefore unlikely to be accidental, (at least if the CO temperature as assumed is a fairly reliable measure of the gas kinetic temperature). It implies some mechanism coupling the kinetic energy of the gas to the infrared radiation, an effect which would readily explain the observed sharp drop-off in the CO temperature beyond the edge of the IR Nebula (Wilson, Jefferts and Penzias 1970). One possibility is that the usual interstellar "cooling" transitions, possibly the J=0 - 2 and J = 1 - 3 H_2 transitions at 28μ and 17μ, are working in reverse near the IR Nebula, absorbing energy from the radiation and transforming it, via collisions, to gas kinetic energy in the molecular cloud. One would expect this mechanism to operate best if all or most of

these transitions are exposed to radiation. The fact that Hoffman et al. (1971) and Harper and Low (1971) have recently found Ori A to be a strongly emitting source even at 100μ would seem to favor this idea.

Penston, Allen and Hyland (1971) have recently suggested that Becklin's IR star is an extremely reddened F supergiant with an absolute visual magnitude, $M_v \sim -8.5$. To explain the observed reddening a visual extinction in front of the star of >80 mag is required, a value which was not considered reasonable until there was evidence for such from these molecular observations. They identify the radiation of the Kleinmann-Low nebula as the reradiation of the energy absorbed in the dust surrounding the star, and derive a mass of the absorbing cloud $\geq 50 M_\odot$ in agreement with that determined from the molecular observations described here.

D. Ortho-Para Ratio

The intensities of the Ori A ortho lines relative to the para can depend on the way in which the molecules are excited, and on the trapping of the 2-mm line radiation; the relative line strengths therefore may depend on T_{kin}, n_{H_2}, and N_{H_2CO}, as well as the ratio of ortho to para molecules. However, assuming that the lines are optically thin and that the ratio of the number of molecules in the J=2 state to the number in the J=1 state is the same for the K=0 and K=1 ladders, the brightness temperatures of the 3 lines are related by (cf. equations (4.6), (4.7) and (4.8))

$$\frac{\left(T_{140}/\nu_{140}\right)+\left(T_{150}/\nu_{150}\right)}{2\left(T_{145}/\nu_{145}\right)} = \frac{N_{ORTHO}}{N_{PARA}} \frac{\begin{pmatrix} 1 & 1 & 2 \\ -1 & 0 & 1 \end{pmatrix}^2}{\begin{pmatrix} 1 & 1 & 2 \\ 0 & 0 & 0 \end{pmatrix}^2} \quad . \qquad (4.28)$$

Taking the results from Table 2 gives the ratio on the left side of the equation (4.28) as 1.9 ± 0.4, yielding

$$\frac{N_{ORTHO}}{N_{PARA}} = 2.5 \pm 0.5 \qquad (4.29)$$

indicating that the observations are consistent with an ortho-para abundance ratio of 3:1.

It should be noted that the conclusions on the ortho-para ratio must be regarded as tentative because of the calibration uncertainties due to double sideband reception (see Appendix A).

E. Collisional Pumping

Averaged over the locations A, B and C listed in Table 2, the mean intensity ratio of the Ori A ortho lines is $T_{140}/T_{150} = 1.0 \pm 0.4$, the uncertainty resulting largely from the uncertainty in calibration. This ratio suggests that the collisional pumping mechanism proposed by Townes and Cheung (1969) to explain anomalous 4.83-GHz absorption in dark nebulae does not operate in the molecular cloud in Ori A, since this scheme posits preferential excitation by neutral impact of the 2_{12} over the 2_{11} level, and hence emission is expected to be more intense at 140 than at 150 GHz. According to White (1970), collisional pumping, if it is to account for the anomalous effect, requires $T_{140}/T_{150} > 1.5$ under the conditions of temperature and density deduced above for the molecular cloud.

Because of the uncertainties, these results are not conclusive, but they emphasized the importance of finding the 4.83-GHz line in Ori A, and the contribution this might make to our understanding of anomalous absorption in dark nebulae. The high densities which have been derived here for the H_2CO cloud would quench the radiative cooling scheme that Thaddeus and Solomon (1972) have proposed to explain this effect, and therefore (if the contention that the molecules are behind Ori A is correct) detection of an absorption line at 4.83 GHz would be strong evidence

for the collisional pumping mechanism proposed by Townes and Cheung (1969). While operation of this mechanism at the relatively high temperature (60 K) of the H_2CO cloud in Ori A might not prove that it was capable of working in dark nebulae (Thaddeus 1972), it would still be of great value as a demonstration that the required cooling action can result from real molecular collisions - a proposition very difficult to prove conclusively either theoretically or in the laboratory.

F. Analysis of the 6-cm Observations

In considering the 6-cm observations in the Orion Nebula, it is notable that the absorption does not show the expected correlation of line intensity T_L with continuum intensity T_C. Thus, as one proceeds from position 17 (Figure 13) off the continuum to the southwest, the line actually increases in intensity, having at position 12 increased in strength 2-1/2 fold, while T_C has declined from 87 K to less than 2 K. This peculiar correlation undoubtedly signifies that it is not the continuum radiation of Ori A which is being absorbed at 6 cm, thus giving further evidence that the observed H_2CO lies behind all or most of the H II region. While one might be tempted to suppose that the 6-cm continuum then comes from a second H II layer still more distant than the H_2CO, this cannot be the case, for to produce the lines in the lower right-hand corner of Figure 13 this layer would of necessity appear as an arm of Ori A with $T_C > 0.5$ K (and considerably greater than 0.5 K, judging from the unsaturated appearance of the line at position 7); as Table 5 shows, no such arm of the nebula is observed. We are thus led to conclude that the microwave background radiation, not H II emission, is being absorbed at 6 cm, and that we are observing from behind the Orion Nebula the "anomalous" line discovered by Palmer et al. (1969) in dark dust clouds.

The continuity in the velocity of the line, and its close

agreement with that of the 2-mm H_2CO emission from the IR nebula, then imply that a more-or-less continuous sheet of material is being observed, extending at least from the vicinity of position 7, where the gas density is presumably rather low, to the very high density ($n_{H_2} \sim 2 \times 10^5$ cm^{-3}) of the IR nebula. This in turn suggests that the decrease in strength of the anomalous line as one proceeds from position 7 to 17 is an effect of increasing neutral particle density. Of course other possible explanations for this decrease exist: it might indicate an increase in the fractional ionization (since the effect of electron impact is to heat the 6-cm transition), or it might only indicate a decline in the density of H_2CO, but analysis of the remarkable self-reversed structure of the line at position 17 (Figure 14) strongly reaffirms the idea that it results from neutral particle impact.

The first point to note in Figure 14 is that no absorption occurs at 8.5 km/sec, corresponding to the 2-mm emission from the IR nebula. This must mean that the anomalous cooling process fails to operate in the IR nebula, since the amount of H_2CO existing there ($N_{H_2CO} \sim 3 \times 10^{14}$ cm^{-2}), according to the 2-mm data, would be expected to produce an easily-detectable ~ 0.15 K absorption line if the excitation temperature T_{ex} of the 6-cm levels were only 1.7 K. There are then two possible interpretations of the self-reversed line profile: (i) it represents 6-cm emis-

sion from the IR nebula superimposed on a broader anomalous line of about the same intensity, presumably produced by outerlying material falling within the 6' antenna beam; or (ii) it represents two separate components of anomalous absorption. (ii) fails to explain why the reversed core of the profile should match so closely both the velocity and width of the 2-mm emission, and it requires an improbable, specific breakdown of the cooling process, with T_{ex} equal to exactly 2.7 K, to explain the absence of a line at 8.5 km/sec. (i) obviously explains the width and velocity of the core, and its observed intensity, $\sim$ 0.12 K, is the expected emission if $N_{H_2CO} \sim 3 \times 10^{14}$ cm^{-2} and $T_{ex} \gg 2.7$ K. (ii) thus requires a rather improbable set of circumstances while (i) does not, and (i) appears to be the more probable interpretation. It is thus concluded that the anomalous pumping process is quenched in the IR nebula, and that 6-cm emission is probably being observed.

It should be noted, however, that due to the uncertainties in the H_2CO column density derived in §B, an expected 6-cm line in the direction of the Kleinmann-Low nebula may be quite weak, and absorption at 8.5 km/sec could be lost in the noise. A test can be suggested which may conclusively confirm that (i) above is the proper explanation. As can be seen from Figure 12 the beam includes the entire observed region of 2-mm emission. It is therefore probable that the source of 6-cm emission does not com-

pletely fill the 6' beam.[1] Therefore, if similar observations are made on a telescope of larger aperture the beam dilution of this source would not be as great, and the resulting emission would appear stronger. It is also possible that more information about this central region will be obtained by using the 140-foot antenna to observe the $2_{11} - 2_{12}$, 2-cm transition, which would be done with a beam width of 2 minutes of arc. These observations will be made in the near future.

In summary, there now appears to be observational evidence that at very high density the pumping process responsible for H_2CO 6-cm anomalous absorption breaks down. This is the expected behavior if the pumping process is radiative, but is contrary to expectation if it is collisional.

---

[1] Judging from how fast the mm lines decrease in intensity in a few minutes of arc, it is not unreasonable to presume that the source of 6-cm emission is beam diluted by a factor of 10 or greater (cf. equation (4.4b)).

G. Analysis of the Silicon Monoxide Observations

The rest frequency of the $J = 3 \rightarrow 2$ SiO transition has not been measured, but it can be calculated from (cf. Herzberg 1945)

$$\nu_{J, J+1} = 2B_o(J+1) - 4D_o(J+1)^3 \quad . \tag{4.30}$$

Taking B_o from the measurement of the frequency of the $J = 0 \rightarrow 1$ transition by Raymonda, Meunter and Klemperer (1970) and using $D_o = 29.8$ kHz (Herzberg 1945, p. 570) gives

$$\nu_{23} = 130\ 268.33 \text{ MHz} \quad , \tag{4.31a}$$

or taking the values of D_e, B_e and α_e ($B_o = B_e - \alpha_e/2$) found by Törring (1968), gives

$$\nu_{23} = 130\ 268.4 \pm 0.3 \text{ MHz} \quad , \tag{4.31b}$$

so these two results agree to 0.14 km/sec. Based on this frequency, the LSR velocity of the line is +53 km/sec, which falls within the range of molecular velocities observed in Sgr B2 and is in agreement with the observed velocities on this source of the millimeter lines of CS (Solomon 1971) and CH_3OH. Thus it appears reasonable to presume

that this new line belongs to SiO. Conclusive confirmation would be provided by detection of the $J = 4 \rightarrow 3$, $2 \rightarrow 1$ or $1 \rightarrow 0$ transitions.[1]

The SiO emission line in Figure 15 is only 13 km/sec wide, and thus much narrower than many molecular lines observed in Sgr B2, particularly those observed at centimeter wavelengths. This difference is probably in part a result of our very high angular resolution, and the marked velocity gradients known to exist over the source (cf. Cheung et al. 1969), but it may also be an indication that distinct chemical or physical inhomogeneities exist in Sgr B2, and that SiO is only produced under quite special conditions, and is not thoroughly mixed throughout the Sgr B2 molecular cloud. It is noteworthy in this regard that $C^{18}O$ (Penzias, Jefferts and Wilson 1971), and OCS and CH_3CN (Solomon et al. 1971), which are the only other molecules so far observed in Sgr B2 at the same angular resolution, have comparable linewidths although they show velocities in the direction of the OH position that are apparently significantly higher (by about 7 km/sec) than that of SiO. It is also possible that the SiO exists over a large region but that the physical conditions required to excite the millimeter transitions into emission exist only in a small region.

---

[1] Since the original writing of this dissertation, Dickinson (private communication) has reported observation of the $J = 2 \rightarrow 1$ SiO transition in the same direction and with the same velocity as the line reported here, thereby confirming the SiO discovery.

Dickinson and Gottlieb (1971) have recently obtained an upper limit of ~1 K on T_R for the 87-GHz, 2→1 line of SiO at our position 1.[1] From the observations reported here, the expected intensity of this line, and that of the J= 1→0 line, as well as the column number density of SiO molecules in Sgr B2, can be estimated. To make these estimates it is necessary to make some assumption as to the excitation temperature of SiO, since these observations cannot distinguish between an optically thin line whose excitation temperature is high, and an optically thick one whose temperature is low.

Because SiO appears to be scarce (Table 7), and because other molecules such as OCS and CH_3CN are well excited in Sgr B2, it is most reasonable to suppose that the J = 3 → 2 transition in Sgr B2 is optically thin, and that its excitation temperature is large with respect to 1.4 K, the radiation temperature T_R of the line in Position 1. To be definite, let us further suppose that as a result of frequent collisions the rotational populations are approximately in equilibrium with the gas kinetic

---

[1] Lower limits were actually quoted, but these authors have found an error in calibration that necessitates doubling the upper limits quoted in Table 1 of their article.

temperature, which is taken to be 30 K. (This assumption may cause an overestimate in the SiO density, but one not likely to exceed a factor of 2-3.)

The column number density in terms of T_R for an optically thin emission line is given by equation (4.18). At the assumed 30 K excitation, the fraction of molecules in the upper level is f= 0.15, 0.12, and 0.085 for the J=3, 2 and 1 levels of SiO respectively. Applying equation (4.18) to the J=3 level, and taking the data from Position 1, then yields

$$N_{SiO} \sim 4 \times 10^{13} \text{ cm}^{-2} \quad , \tag{4.32}$$

which is 10-100 times less than the formaldehyde column density in Sgr B2 (Zuckerman et al. 1970). If equation (4.18) is applied to the J=2 and J=1 levels, and equation (4.32) is used for N_{SiO}, we find that

$$T_R (2 \rightarrow 1) \sim 0.6 \text{ K} \tag{4.33}$$

and

$$T_R (1 \rightarrow 0) \sim 0.16 \text{ K} \quad . \tag{4.34}$$

Equation (4.33) would correspond to an antenna temperature of ~ 0.3 K and is evidently consistent with the negative result of Dickinson and Gottlieb (1971); it and equation (4.34) suggest that the lower frequency lines of SiO may not be easy to detect. Alternately, if these lines are found to be more intense than equations (4.33) and (4.34) indicate, this estimate of the SiO excitation and density will require some revision.

Applying the above treatment to the J=4→3 transitions yields

$$T_R (4 \rightarrow 3) \sim 2.5 \text{ K} \quad . \tag{4.35}$$

This implies that this line at $\nu = 173.661$ GHz might be more easily detectable. A search for this line could confirm the identification and might lead to the discovery of SiO in other locations.

There are a number of observations of SiO which would be of interest for the future. These would include a search for other transitions, a search for SiO in the direction of late type stars (Knacke et al. 1969; Fertel 1970; Cudaback, Gaustad and Knacke 1971); and infrared objects such as VY Ca M (Gillett, Stein and Solomon 1970) where vibration-rotation bands of SiO have been reported.

CHAPTER V

SUMMARY AND CONCLUSIONS

The following summarize the salient results and conclusions of this dissertation.

Three new rotational transitions of formaldehyde, one belonging to the previously undetected para species of the molecule, have been observed at wavelengths of $\sim$ 2 mm. All three lines were detected in the direction of the Kleinmann-Low nebula in the Orion Nebula, and the 140.8-GHz line was mapped over an area $\sim$ 3' x 5' in this region. Also, useful upper limits were obtained for the 146.6- and 137.4-GHz lines of $H_2{}^{13}CO$. It was concluded that the 2-mm H_2CO emission results from neutral particle impact, most likely with H_2 molecules. The H_2 density required to produce the $\sim$ 7 K emission has been estimated to be $\sim 2 \times 10^5$ cm^{-3}, corresponding to a total mass in the central region of the Kleinmann-Low nebula of $\sim 230 M_\odot$. This high density also implies an optical extinction of about 200 magnitudes.

The 140.8-GHz line was also observed in five other sources: Sgr A (NH_3A), W3(OH), W51, DR 21 (OH) and Ori B. The velocities and widths of the 140.8-GHz line are in agreement with those of the millimeter lines of CS and HCN observed in the first four of these sources. Since the densities required to excite the millimeter lines

in these three molecules are comparable, this supports the conclusion that the excitation of these transitions is collisional.

Weak absorption from the 6-cm H_2CO line was observed over most of the Orion Nebula. The line strength shows a negative correlation with continuum intensity and at the fringe of the Orion Nebula it is more intense than the continuum, indicating that "anomalous" absorption, similar to that found by Palmer et al. (1969) in dark clouds, is being observed. In the direction of the Kleinmann-Low nebula the line appears self-reversed, providing observational evidence that at very high density the pumping process breaks down, and that we may, in fact, be observing 6-cm emission. This breakdown of the pumping mechanism is expected if the mechanism is radiative.

The combination of the 2-mm and 6-cm observations has yielded further information on the nature and location of the Kleinmann - Low nebula. The observations strongly suggest a cloud located behind the H II region and extending on all sides beyond the visible portions of the nebula. The central portion of this nebula is of high density and appears to contain the OH emission source, the IR nebula and the IR star, which is probably the central condensation of the cloud (Penston, Allen and Hyland 1971).

The $J = 3 \rightarrow 2$ transition of silicon monoxide was detected in the direction of Sgr B2 at a frequency of 130.4 GHz. The observed line is narrower than previously observed molecular lines in this source, but the width is in agreement with that of other millimeter lines found in Sgr B2. This was taken to support the conclusion that these millimeter transitions are collisionally excited and that the lines are most visible in regions of high density.

Perhaps the most significant conclusion reached in this dissertation is that the millimeter wavelength emission lines of H_2CO and presumably those of similar molecules, result from neutral particle impact, most plausibly with hydrogen molecules, in regions where the density and extinction are extremely high. It is therefore expected that these millimeter lines will be particularly useful in the study of these dense regions.

Finally, these observations provide a number of suggestions for future work. The accurate determination of the relative intensities of the three 2-mm H_2CO lines, using calibration spectra, would yield information on the pumping mechanism and the ortho - para ratio, the latter being related to the temperature of formation of the formaldehyde. The use of an antenna with a higher angular resolution at 6-cm than the 140-foot telescope to observe the 6-cm H_2CO line in the direction of the Kleinmann - Low nebula could confirm the interpretation of

the self-reversed feature observed there as 6-cm formaldehyde emission. Also, a search for the 2-cm H_2CO line in Ori A would be important. If this line were found, we would then have, from one region, observations of the four allowed transitions connecting the four lowest ortho - H_2CO levels. Finally, finding the $J = 4 \rightarrow 3$ SiO transition would confirm the discovery of SiO and would yield more information on the excitation of this molecule.

APPENDIX A

KITT PEAK RECEIVER CALIBRATION

The receiver was calibrated at least as often as every two hours and whenever a new source was acquired. This was accomplished by alternately viewing "cold" sky at the same elevation angle, θ, as the source, and either a room temperature absorbed placed in front of the feed horn, or noise from a breakdown diode injected into the receiver via a directional coupler (Figure 2). These calibration signals are obviously broad band, and enter the receiver through both the signal and the image sidebands. Let g_s and g_i be the respective mixer gains for these two sidebands, and let $f = g_s/(g_s+g_i)$. Then this calibration procedure is equivalent to injecting into the signal sideband only radiation at a temperature

$$T_{CAL} = \frac{T_o - T_{SKY}(\theta)}{f} \qquad (A1)$$

where $T_{SKY}(\theta)$ is the "cold" sky temperature and was determined from antenna tipping (see Appendix B) and T_o is the temperature of the absorber or noise source. The major calibration problem comes from the fact that the mixer response in the two sidebands is not in general the same, being sensitive to the tuning of the mixer. Therefore, f is not precisely known; repeated line observations in a given location indicate that it may vary by as much as 25%.

Calibration changes at one frequency can be checked by periodically remeasuring a line at one location, but unfortunately, the relative intensities of lines at different frequencies and the absolute intensity of any line can currently be determined only to within the 25% mentioned above.

A new calibration method is currently being tested. Calibration spectra will be obtained from cells, containing samples of the molecule under investigation. The use of calibration spectra, well-known in optical astronomy, has the obvious advantage in this case that the calibration signal enters only through one sideband.

APPENDIX B

CORRECTION FOR ATMOSPHERIC ATTENUATION

B1. Theory

At a wavelength of 2 mm, atmospheric attenuation, mainly by water vapor, is significant. Correction for it is made on the assumption that the absorption occurs in a plane parallel layer at constant temperature, T_{AT}, and that the optical depth looking through the atmosphere at an elevation, θ, is

$$\tau(\theta) = \tau_o \csc\theta \tag{B1}$$

where τ_o is the zenith opacity. Then, if the true line temperature is T_L, the observed line temperature will be

$$T_{OBS} = T_L e^{-\tau_o \csc\theta} . \tag{B2}$$

To find τ_o consider the following:

If the antenna is pointed at "cold" sky the antenna temperature is

$$T_A(\theta) = T_{AT}\left(1 - e^{-\tau(\theta)}\right) + T_B e^{-\tau(\theta)} + T_G(\theta) \tag{B3}$$

where T_B is the background temperature and is much less than T_{AT}, and $T_G(\theta)$ is ground radiation entering through side lobes, so

$$T_A(\theta) - T_G(\theta) \approx T_{AT}\left(1 - e^{-\tau_o \csc \theta}\right) . \qquad \text{(B4)}$$

If we look at two elevations, θ_1, and θ_2, we have

$$\frac{T_{AT} - T_A(\theta_1) + T_G(\theta_1)}{T_{AT} - T_A(\theta_2) + T_G(\theta_2)} = e^{-\tau_o(\csc \theta_2 - \csc \theta_1)} \qquad \text{(B5)}$$

or

$$\tau_o = \left(\csc \theta_2 - \csc \theta_1\right)^{-1} \ell n \left[\frac{T_{AT} - T_A(\theta_1) + T_G(\theta_1)}{T_{AT} - T_A(\theta_2) + T_G(\theta_2)} \right] . \qquad \text{(B6)}$$

B2. Antenna Tipping

The antenna was pointed at "cold" sky at a number of elevations and the total power was recorded. To calibrate the total power scale two loads were placed in front of the feed, one at the ambient temperature and the other dipped in liquid nitrogen.

Specification of $T_G(\theta)$ requires detailed knowledge of the side lobe pattern which was not available. However, from the tipping data, T_G appears to vary from about 25 K to 40 K, so it has been assumed that T_G = 30 K for all angles, which may introduce an error of at most 10 K. For comparison angles not too close together an uncertainty in T_G of 10 K would produce an uncertainty in τ_o of about 0.003. (For typical values of τ_o this is a 5% error.)

For an error $\Delta\tau_o$ in the determination of τ_o, the resulting error in the derived value of T_L for any observation is given by

$$\frac{\Delta T_L}{T_L} = \Delta\tau_o \csc\theta \qquad \text{(B7)}$$

so for $\theta > 20°$, an error of 0.003 in τ_o would cause an error in T_L of at most 1%.

APPENDIX C

LINE BROADENING BY THE FILTERS

The effect of the finite width of the filters on the observed linewidths can be estimated by assuming that both the filter passbands and the actual line shape are gaussian with FWHM of σ_f and σ_ℓ, respectively. Then the observed line will also be gaussian with a width σ_o given by

$$\sigma_o = \sqrt{\sigma_f^2 + \sigma_\ell^2} \quad . \tag{C1}$$

Since the actual width of the line is less than the observed width, the actual maximum intensity must be greater than that observed, i.e., if T_o is the observed intensity then the actual intensity is given by

$$T_\ell = \frac{T_o \sigma_o}{\sigma_\ell} \quad . \tag{C2}$$

ACKNOWLEDGEMENTS

I wish to express my special appreciation to Professor Patrick Thaddeus who has been my advisor on this project. I have benefited greatly from his guidance and scientific counsel.

My thanks go to Dr. Robert Jastrow for his hospitality at the NASA Goddard Institute for Space Studies and for the generous grants of computer time necessary for the data analysis.

I especially thank Drs. Arno A. Penzias, Robert W. Wilson and Keith B. Jefferts of the Bell Telephone Laboratories for the unique opportunity to join with them in the use of their millimeter receiver.

I gratefully acknowledge the National Radio Astronomy Observatory for grants of observing time and the crews of the 36-foot and 140-foot telescopes for their assistance with the observations.

For their efforts in typing various stages of this manuscript, I would like to thank Miss Josephine Koller, the rest of the Technical Typing staff and Miss Margaret Kavanau. Mr. Theodore Psaropulos prepared many of the illustrations and I acknowledge the assistance of many others on the staff of the Goddard Institute.

I am grateful for the support of the Columbia University Physics Department and I was also fortunate to be a National Science Foundation Graduate Fellow.

I would also like to thank Messrs. J.A. Grange, R.B. Nerf, E.S. Palmer, N.Z. Scoville and M.A. Sonnenberg and Drs. J.F. Moore and J.M. Pasachoff for their assistance, useful conversations and friendship.

I am, naturally, appreciative of the encouragement I received from my parents throughout my education.

I wish to express my deepest appreciation to my versatile wife, Nancy, for her invaluable assistance in programming, typing, preparation of illustrations and critical analysis of the drafts of this thesis and most of all, for her constant moral support.

REFERENCES

Adams, W. S. 1949, Ap. J., 109, 335.

Allison, A. C., and Dalgarno, A. 1971, Astronomy and Astrophysics, 13, 331.

Auer, L. H., and Mihalas, D. 1969, Ap. J., 158, 641.

_____ 1970, M. N. R. A. S., 149, 65.

Ballister, M. 1968, The NRAO 50-Channel Spectral Line Receiver, NRAO EDIR No. 70.

Becklin, E. E., and Neugebauer, G. 1967, Ap. J., 147, 799.

Bortolot, V. J., Jr. 1972, unpublished dissertation, New York Univ.

Bortolot, V.J., Jr., and Thaddeus, P. 1969, Ap. J. (Letters), 155, L17.

Carruthers, G. R. 1970, Ap. J. (Letters), 161, L81.

Cheung, A. C., Rank, D. M., Townes, C. H., Thornton, D. D., and Welch, W. J. 1968, Phys. Rev. Letters, 21, 1701.

Cheung, A. C., Rank, D. M., Townes, C. H., Knowles, S. H., and Sullivan, W. T. 1969, Ap. J. (Letters), 157, L13.

Clauser, J. F. 1969, unpublished dissertation, Columbia Univ.

Cudaback, D. D., Gaustad, J. E., and Knacke, R. F. 1971, Ap. J. (Letters), 166, L49.

Dickinson, D. F., and Gottlieb, C. A. 1971, Astrophys. Letters, 7, 205.

Dieter, N. 1971 (private communication).

Evans, N. J., Cheung, A. C., Sloanaker, R. M. 1970, Ap. J. (Letters), 159, L9.

Farris, S., Greenhalgh, A., and Vitiello, D. 1968, Integration System of Computer Programs for the 413-Channel Autocorrelation Receiver, NRAO EDIR No. 5.

Fertel, J. H. 1970, Ap. J. (Letters), 159, L7.

Gardner, F. F., Ribes, J. C., and Cooper, B. F. C. 1971, I. A. U. Circular No. 2354.

Gardner, F. F., and Whiteoak, J. B. 1970, Astrophys. Letters, 5, 161.

Gaustad, J. 1963, Ap. J., 138, 1050.

Gillett, F. C., Stein, W. A., and Solomon, P. M. 1970, Ap. J. (Letters), 160, L173.

Gordon, M. A., and Meeks, M. L. 1968, Ap. J., 152, 417.

Harper, D. A., and Low, F. J. 1971, Ap. J. (Letters), 165, L9.

Hartmann, W. K. 1967, Ap. J. (Letters), 149, L87.

Herzberg, G. 1945, Infrared and Raman Spectra (New York: D. Van Nostrand Company, Inc.).

Hoffman, W. F., Frederick, C. L., and Emery, R. J. 1971, Ap. J. (Letters), 170, L89.

Hollenbach, D. J., Werner, M. W., and Salpeter, E. E. 1970, Ap. J., 163, 165.

Hulst, H. C., van de. 1949, Rech. Astr. Obs. Utrecht, 11, Part 2.

Jefferts, K. B., Penzias, A. A., and Wilson, R. W. 1970, Ap. J. (Letters), 161, L87.

Jefferts, K. B., Penzias, A. A., Wilson, R. W., and Solomon, P. M. 1971, Ap. J. (Letters), 168, L111.

Kerr, F. J. 1968, Stars and Stellar Systems, (University of Chicago Press), 7, Chapter 10.

Kleinmann, D. E., and Low, F. J. 1967, Ap. J. (Letters), 149, L1.

Knacke, R. F. 1968, Nature, 217, 44.

Knacke, R. F., Gaustad, J. E., Gillett, F. C., and Stein, W. A. 1969, Ap. J. (Letters) 155, L189.

Knowles, S. H., Mayer, C. H., Cheung, A. C., Rank, D. M., and Townes, C. H. 1969, Science, 163, 1055.

Krishna Swamy, K. S. 1971, Astronomy and Astrophysics, 14, 405.

Kutner, M. L. 1972, Proc. NRAO Symposium on Interstellar Molecules (to be published).

Kutner, M., and Thaddeus, P. 1971, Ap. J. (Letters), 168, L67.

Kutner, M., Thaddeus, P., Jefferts, K. B., Penzias, A. A., and Wilson, R. W. 1971, Ap. J. (Letters), 164, L49.

Litvak, M. M. 1970, Ap. J. (Letters), 160, L133.

Meeks, M. L. 1971 (private communication).

Mezger, P. G., and Henderson, A. P. 1967, Ap. J., 147, 471.

Nerf, R. 1972 (to be published).

Ney, E. P., and Allen D. A. 1969, Ap. J. (Letters), 155, L193.

Oka, T. 1970, Ap. J. (Letters), 160, L69.

Palmer, P., and Zuckerman, B. 1967, Ap. J., 148, 727.

Palmer, P., Zuckerman, B., Buhl, D., and Snyder, L. E. 1969, Ap. J. (Letters), 156, L147.

Penner, S. S. 1959, Quantitative Molecular Spectroscopy and Gas Emissivities (Addison-Wesley).

Penston, M. V., Allen, D. A., and Hyland, A. R. 1971, Ap. J. (Letters), 170, L33.

Penzias, A. A., Jefferts, K. B., and Wilson, R. W. 1971, Ap. J., 165, 229.

Penzias, A. A., Solomon, P. M., Wilson, R. W., and Jefferts, K. B. 1971, Ap. J. (Letters), 168, L53.

Raimond, E., and Eliasson, B. 1967, Ap. J. (Letters), 150, L171.

_____ 1969, Ap. J., 155, 817.

Rank, D. M., Townes, C. H., and Welch, W. J. 1971, Science, 174, 1083.

Raymonda, J. W., Muenter, J. S., and Klemperer, W. A. 1970, J. Chem. Phys., 52, 3458.

Schraml, J., and Mezger, P. G. 1969, Ap. J., 156, 269.

Scoville, N. Z., Solomon, P. M., and Thaddeus, P. 1972, Ap. J. (in press).

Shalloway, A. M., Mauzy, R., Greenhalgh, J., Weinreb, S. 1968, Autocorrelation Receiver - Model II; Operational Description, NRAO EDIR No. 75.

Smith, A. M., and Stecher, T. P. 1971, Ap. J. (Letters), 164, L43.

Snyder, L. E., and Buhl, D. 1971, Ap. J. (Letters), 163, L47.

Snyder, L. E., Buhl, D., Zuckerman, B., and Palmer, P. 1969, Phys. Rev. Lett., 22, 679.

Solomon, P. M. 1971 (private communication).

Solomon, P. M., Jefferts, K. B., Penzias, A. A., and Wilson, R. W. 1971, Ap. J. (Letters), 168, L107.

Spitzer, L. 1968, Stars and Stellar Systems, 7, 1.

Stief, L. J. 1971 (private communication).

Thacker, D. L., and Beale, L. 1969, Multifilter Receivers, NRAO EDIR No. 88.

Thaddeus, P. 1972, Ap. J. (in press).

Thaddeus, P., and Solomon, P. M. 1972 (to be published).

Thaddeus, P., Wilson, R. W., Kutner, M., Penzias, A. A., and Jefferts, K. B. 1971, Ap. J. (Letters), 168, L59.

Törring, T. 1968, Z. Naturforsch, 23A, 777.

Townes, C. H., and Cheung, A. C. 1969, Ap. J. (Letters), 157, L103.

Townes, C. H., and Schawlow, A. L. 1955, Microwave Spectroscopy (New York: McGraw Hill Book Company, Inc.).

Tucker, K. D., Tomasevich, G. R., and Thaddeus, P. 1970, Ap. J. (Letters), 161, L153.

Vanden Bout, P., and Thaddeus, P. 1971, Ap. J., 170, 297.

Weinreb, S., Barrett, A. H., Meeks, M. L., and Henry, J. C. 1963, Nature, 200, 829.

Weinreb, S. 1963, A Digital Spectral Analysis Technique and its Application to Radio Astronomy, dissertation, MIT.

———— 1970, Millimeter-Wave Spectral-Line Receiver - Local Oscillator and IF Sections, NRAO EDIR No. 97.

Welch, W. J. 1970, B. A. A. S., 2, 355.

White, R. E. 1970, unpublished dissertation, Columbia University.

Whiteoak, J. B., and Gardner, F. F. 1970, Astrophys. Letters, 5, 5.

Wilson, O. C., Munch, G., Flather, E. M., and Coffeen, M. F. 1959, Astrophysical Journal Supplement, 4, 199.

Wilson, R. W., Jefferts, K. B., and Penzias, A. A., 1970, Ap. J. (Letters), 161, L43.

Wilson, R. W., Penzias, A. A., Jefferts, K. B., Kutner, M., and Thaddeus, P. 1971, Ap. J. (Letters), 167, L97.

Zuckerman, B., Buhl, D., Palmer, P., and Snyder, L. E. 1970, Ap. J., 160, 485.

Zuckerman, B., Palmer, P., Snyder, L. E., and Buhl, D. 1969, Ap. J. (Letters), 157, L167.

TABLE 1. H_2CO LINE REST FREQUENCIES

ISOTOPIC SPECIES	TRANSITION	REST FREQUENCY (MHz)	REFERENCE
$H_2{}^{12}CO$	$1_{11} - 1_{10}$	4829.65996 ±0.00005	1
	$2_{12} - 1_{11}$	140839.53 ±0.03	2
	$2_{11} - 1_{10}$	150498.36 ±0.03	2
	$2_{02} - 1_{01}$	145602.97 ±0.03	2
$H_2{}^{13}CO$	$2_{12} - 1_{11}$	137449.97 ±0.03	2
	$2_{11} - 1_{10}$	146635.69 ±0.03	2
	$2_{02} - 1_{01}$	141983.75 ±0.03	2

References: (1) Tucker, Tomasevich and Thaddeus (1970).

(2) Nerf (1972).

TABLE 2: SUMMARY OF 2-MM FORMALDEHYDE OBSERVATIONS IN THE ORION NEBULA

Location on Map	α(1950)	δ(1950)	140.8 GHz		145.6 GHz		150.5 GHz	
			T_A (° K)	v_{LSR} (km/sec)	T_A (° K)	v_{LSR} (km/sec)	T_A (° K)	v_{LSR} (km/sec)
	$5^h\ 32^m\ 52.9^s$	-5° 23'54.4"	0.9	8.0				
	5 32 50.9	-5 23 54.4	1.9	8.5	1.1	7.5	<0.7	—
	5 32 50.9	-5 24 24.4	1.1	9.5				
	5 32 50.9	-5 24 54.4	1.2	9.0				
	5 32 50.9	-5 25 24.4	1.0	8.5				
	5 32 50.9	-5 26 24.4	<0.5	—				
	5 32 48.9	-5 23 54.4	2.4	8.0	1.6	9.5		
	5 32 48.9	-5 25 24.4	2.1	8.5				
A	5 32 46.9	-5 22 54.4	1.4	8.5	0.7	9.0	1.8	8.5
	5 32 46.9	-5 23 24.4	2.5	9.5				
B*	5 32 46.9	-5 23 54.4	3.0	8.5	1.5	9.5	2.6	8.5
	5 32 46.9	-5 24 24.4	3.6	8.5				
	5 32 46.9	-5 24 54.4	2.6	8.0	2.4	8.0		
C†	5 32 46.9	-5 25 24.4	2.8	7.5	1.9	7.5	2.7	7.5
	5 32 46.9	-5 25 54.4	3.1	7.0				
	5 32 46.9	-5 26 24.4	2.1	7.5	1.6	7.5		
	5 32 46.9	-5 26 54.4	1.5	8.0				
	5 32 44.9	-5 23 54.4	1.6	8.0			2.4	8.5
	5 32 44.9	-5 25 24.4	1.9	7.5				
	5 33 42.9	-5 23 54.4	1.5	7.5				
	5 33 42.9	-5 24 24.4	1.2	8.0				
	5 33 42.9	-5 25 24.4	1.0	8.0				
	5 32 40.9	-5 23 54.4	1.2	8.5				
	5 32 38.9	-5 23 54.4	1.0	8.5				

*Upper limit $T_A < 0.1$ K obtained at this position for the 137.4-GHz $H_2{}^{13}CO$ line.

†Upper limit $T_A < 0.2$ K obtained at this position for the 146.6-GHz $H_2{}^{13}CO$ line.

TABLE 3.

140.8 GHz H_2CO NEGATIVE RESULTS

Object	α(1950)	δ(1950)	Velocity Range† (km/sec)	Integration Time (min)	Upper Limit on T_A(K)*
W3	$2^h 23^m 16^s$	61°38′55″	-110 to +16	15	1.1
	2 23 16	61 39 55		5	1.1
	2 23 16	61 37 55		5	1.3
	2 23 20	61 38 55		10	1.0
	2 23 12	61 38 55		10	1.0
Taurus Cloud(1)	4 29 46	24 17 32	- 58 to +68	20	0.6
	4 29 16	24 17 32		20	0.7
Cloud 2(1)	4 38 27	25 17 47	- 58 to +68	30	0.6
Horsehead	5 38 39	- 2 28 01	- 54 to +72	10	0.9
NGC 2024	5 39 13	- 1 55 18	- 54 to +72	40	0.6
Sgr A	17 42 26	-28 56 47	+ 37 to +163	45	0.7
Sgr B2	17 44 10	-28 22 47	- 1 to +125	20	0.5
M17	18 17 34	-16 12 31	- 40 to +86	45	0.8
W49	19 07 59	9 00 06	- 53 to +73	5	0.9
	19 07 55	9 00 06		5	1.4
	19 07 51	9 00 06		5	1.5
	19 07 47	9 00 06		5	1.3
	19 07 43	9 00 06		5	1.1
	19 07 39	9 00 06		5	1.4
	19 07 35	9 00 06		5	1.5
	19 07 59	8 59 06		5	1.6
	19 07 55	8 59 06		5	1.6
	19 07 51	8 59 06		5	1.5
	19 08 47	9 00 45		20	1.1
	19 08 47	9 01 45		5	1.2
	19 08 47	8 59 45		5	1.4
	19 08 51	9 00 45		5	1.2
	19 08 43	9 00 45		5	1.5
W51	19 22 28	14 23 16	+ 1 to +127	5	1.1
	19 22 32	14 24 16		5	1.3
	19 22 24	14 24 16		5	1.5
	19 22 30	14 29 05		5	1.0
DR21	20 37 12	42 09 12	- 68 to +58	20	2.0

* Corresponds to 4 standard deviations of the noise.

† In the local standard of rest.

(1) Regions of anomalous 4.83 GHz absorption

TABLE 4.

140.8 GHz EMISSION IN OTHER SOURCES

Source*	α(1950)	δ(1950)	T_A(°K)	v_{LSR} (km/sec)	$\Delta v^\dagger$ (km/sec)
W3(OH)	$2^h\ 23^m\ 09^s$	+61°39'00"	0.3	-45.5	9
	2 23 17	+61 38 00	0.5	-47.5	10
→	2 23 17	+61 39 00	0.8	-48.0	7
	2 23 17	+61 40 00	0.3	-50.5	10
	2 23 25	+61 38 00	0.3	-50.5	7
	2 23 25	+61 39 00	0.3	-50.0	12
Ori B	5 39 12	-1 55 42	1.0	+9.0	4
Sgr A(NH_3A)	17 42 28.0	-29 01 30	0.8	+19.0	24
W51	19 21 23	+14 24 30	0.8	+59.4	9
	19 21 27	+14 23 30	0.6	+55.4	12
→	19 21 27	+14 24 30	1.5	+53.4	11
	19 21 27	+14 25 30	0.8	+52.4	11
	19 21 31	+14 24 30	0.5	+52.0	—
DR 21(OH)	20 37 11	+42 12 00	1.2	-3.0	8
	20 37 14	+42 11 30	0.7	-3.0	7.5
	20 37 14	+42 12 00	1.5	-3.0	7.5
	20 37 14	+42 12 30	0.5	-4.0	7.5
	20 37 17	+42 12 00	0.4	-3.0	8

*Arrows indicate location of lines shown in Figure 3.

† Line width at half intensity.

TABLE 5.

SUMMARY OF 6-CM H_2CO OBSERVATIONS IN ORI A

Position number	α(1950)	δ(1950)	T_L (°K)	v_{LSR} (km/sec)	Δv (km/sec)	T_c (°K)
(1)	(2)	(3)	(4)	(5)	(6)	(7)
1	$5^h 31^m 36.0^s$	-5°48'00"	< 0.15	-	-	< 0.41*
2	5 31 36.0	-5 54 00	< 0.15	-	-	< 0.41*
3	5 31 36.0	-6 00 00	~ 0.1(?)	9	-	< 0.41*
4	5 32 00.0	-5 36 00	0.33	8.5	3	< 2.4
5	5 32 00.0	-5 42 00	0.35	8	3	< 0.41*
6	5 32 00.0	-5 48 00	0.36	9	3	< 0.41*
7	5 32 00.0	-5 54 00	0.50	9.5	1.5	< 0.41*
8	5 32 00.0	-6 00 00	~ 0.1	9.5	2	< 0.41*
9	5 32 22.0	-5 16 00	0.1	9	7	< 2.4
10	5 32 24.0	-5 24 00	0.16	9.5	6	30
11	5 32 24.0	-5 30 00	0.18	9	5	10
12	5 32 24.0	-5 36 00	0.25	8.5	5	< 2.4
13	5 32 24.0	-5 42 00	0.48	8	4	< 0.41*
14	5 32 24.0	-5 48 00	0.50	8	4	< 0.41*
15	5 32 34.0	-5 12 00	< 0.2	-	-	< 2.4
16	5 32 46.0	-5 16 00	0.15	9	6	3.5
17	5 32 46.7	-5 23 56	~ 0.1 –	See text		87
18	5 32 48.0	-5 30 00	~ 0.05	9	~ 4	25
19	5 32 48.0	-5 48 00	~ 0.1	8.5	6	< 0.41*
20	5 33 10.0	-5 16 00	0.15	9	-	2.5
21	5 33 10.0	-5 22 00	< 0.2	-	-	6
22	5 33 10.0	-5 28 00	< 0.15	-	-	6
23	5 33 10.0	-5 34 00	0.10	16	5	< 2.4
24	5 33 34.0	-5 16 00	< 0.15	-	-	< 2.4
25	5 33 34.0	-5 22 00	~ 0.1	9	~ 4	< 2.4
26	5 33 58.0	-5 22 00	~ 0.1	9	~ 4	< 2.4

* M. L. Meeks (1971).

TABLE 6. SiO in SGR B2

Position	α(1950)	δ(1950)	T_A(°K)	v_{LSR}(km/sec)	Δ v(km/sec)*
1	$17^h\ 44^m\ 09.6^s$	-28° 22' 25"	0.7	52	13
2	17 44 05.0	-28 22 06	~0.7	47	12

* Full linewidth at half intensity.

TABLE 7. SUMMARY OF SiO NEGATIVE RESULTS

Source	α(1950)	δ(1950)	LSR Velocity Range (km/sec)	Upper Limit on T_A(°K)*
Ori A	$5^h\ 32^m\ 46.9^s$	-5° 23' 56"	-60 to +55	0.4
IRC + 10216	9 45 14.8	13 30 40	-104 to +80	0.5
Sgr A(NH_3A)	17 42 28.0	-29 01 30	-31 to +153	0.4
W51	19 21 27.0	14 24 30	-1 to +113	0.5
DR21(OH)	20 37 13.9	42 12 00	-58 to +56	0.8
NML Cyg	20 44 33.0	39 56 06	-60 to +124	1.2

* Peak-to-peak noise.

FIGURE CAPTIONS

Figure 1: The lowest lying formaldehyde energy levels. The four transitions reported in this dissertation are indicated.

Figure 2: Schematic diagram of the Kitt Peak receiver. For klystron frequency stabilization the 2-GHz oscillator (8) is locked to the 20^{th} harmonic of the frequency synthesizer (7) and the N^{th} harmonic of this is then mixed with ν_{LO}. (The harmonic mixer (10) as well as the signal mixer (3) uses Schottky barrier diodes.) This signal is then compared with f_2, and if there is any difference a correction signal is sent to the klystron (6). Frequency switching is accomplished by switching f_2 between the two 400 MHz oscillators, set at f_2^{sig} and f_2^{ref}.

Figure 3: The three $J = 2 \rightarrow 1$ H_2CO lines in Ori A at the location indicated "C" in Figure 6.

Figure 4: Map of 140.8-GHz formaldehyde emission in Ori A. Observations were taken at an angular separation of 1', with the antenna pointing towards the centers of the squares. The observed antenna temperatures are given in 4a, which also shows the isophotes of antenna temperature for the 1.95-cm continuum radiation (Schraml and Mezger 1969). Figure 4b shows the location of the map in 4a with respect to the infrared nebula (Ney and Allen 1969), the infrared star and OH source, and the trapezium stars. The

60" half power beam width (HPBW), extrapolated from the HPBW at 115 GHz, is indicated by the solid circle and the 90" upper limit to the HPBW, obtained from scans across the moon's limb, is indicated by the dotted circle. (This map was made in October, 1970).

Figure 5: Extended map of 140.8-GHz H_2CO emission in Ori A. The center of each box is the direction of observation and each box is approximately half a beam width across. The indicated vertical scale for the spectra (baseline to top of box) is 5 K in T_A. The horizontal scale marks indicate LSR radial velocities of 0, 10, and 20 km/sec. (This map was made in February, 1971).

Figure 6: Contour map of 140.8-GHz H_2CO emission in Ori A, made from the observations shown in Figure 5, shown in relation to the IR star of Becklin and Neugebauer (1967), the point source of OH emission (Raimond and Eliasson 1967) and the continuum peak of the IR nebula. No correction has been made for the beam width of the antenna.

Figure 7: Map of 150.5-GHz formaldehyde emission in Ori A. Scales for the spectra are as in Figure 5.

Figure 8: Map of 145.6-GHz para-formaldehyde emission in Ori A. Vertical scale for the spectra is 3 K in T_A and all other scales are as in Figure 5.

Figure 9: Profiles of 140.8-GHz emission in Sgr A (NH_3A), W3 (OH) and W51, at the locations indicated in Table 4. Published profiles of HCN 88-GHz emission (Snyder and Buhl 1971) and H_2CO 4.83-GHz absorption (Zuckerman et al. 1970), not drawn to the same intensity scale, and inverted in the case of 4.83 GHz, are shown for comparison.

Figure 10: Map of 140.8-GHz formaldehyde emission in W51. Each box is approximately a beamwidth in size. The vertical scale for the spectra is 2 K in T_A. The horizontal scale marks indicate LSR velocities of 40, 50 and 60 km/sec.

Figure 11: Map of 140.8-GHz formaldehyde emission in W3 (OH). Each box is approximately a beamwidth in size. The vertical scale for the spectra is 1 K in T_A. The horizontal scale marks indicate LSR radial velocities of -40, -50 and -60 km/sec.

Figure 12: Photograph of the Orion Nebula showing the locations of the 6-cm observations, the circles being roughly the size of the HPBW (6'). The T_A = 2.5 and 1.0 K contours of 2-mm emission (Figure 6) are shown in location 17, the location of the 6-cm continuum peak and the IR nebula. (Lick Observatory photograph.)

Figure 13: Map of the 6-cm line profiles. The center of each box is the direction of observation, and each box is approximately the size of the antenna beamwidth. The full vertical scale of the spectra is 0.8 K in T_B, unless indicated by X2 or X4, where it is respectively 0.4 and 0.2 K. The three horizontal scale marks indicate LSR radial velocities of 0, 10 and 20 km/sec.

Figure 14: Comparison of the 6-cm and the 2-mm line profiles in the direction of the IR nebula, location 17. The 6-cm profile is an enlargement of that in Figure 13 and represents a total integration of 420 min. The wide 2-mm profile is the observed 140.8-GHz line shown in Figure 3; the narrow one is a reconstruction of actual width of this line made by assuming that both the unfiltered line and the 2-MHz filters in the receiver are Gaussian in shape (cf. Appendix C).

Figure 15: The $J = 3 \rightarrow 2$ transition of silicon monoxide in Sgr B2 - position 1 in Table 6. The radial velocity and frequency scales are with respect to the local standard of rest. Observations were made on 27 April 1971. Only 35 channels are shown, since two sets of data, taken with the receiver frequency shifted by 5 MHz, have been added together.

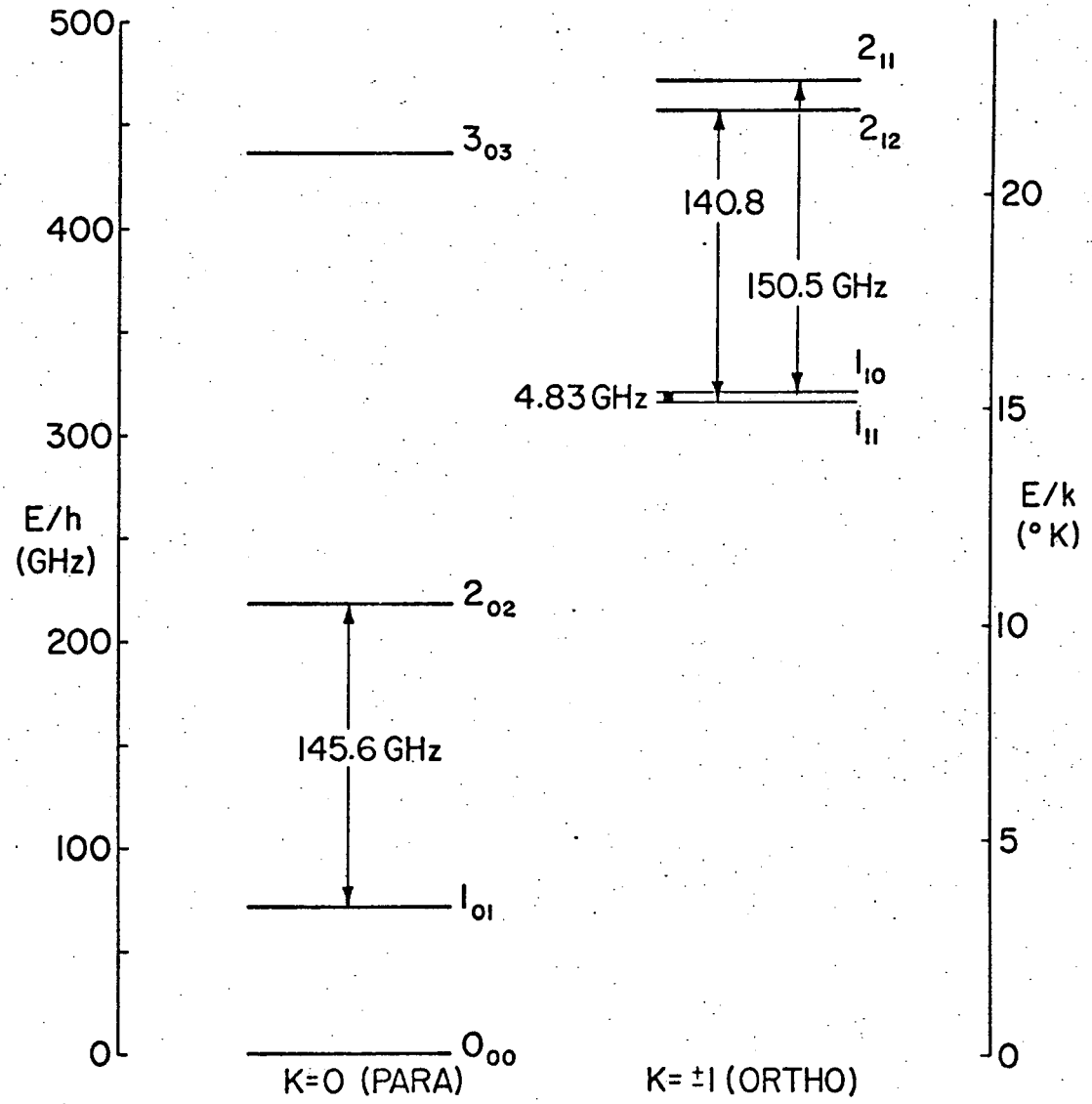
500
400
300
200
100
0
E/h
(GHz)
3_{03}
2_{02}
145.6 GHz
1_{01}
0_{00}
K=0 (PARA)
2_{11}
2_{12}
140.8
150.5 GHz
1_{10}
4.83 GHz
1_{11}
K= ±1 (ORTHO)
20
15
10
5
0
E/k
(° K)

Figure 1

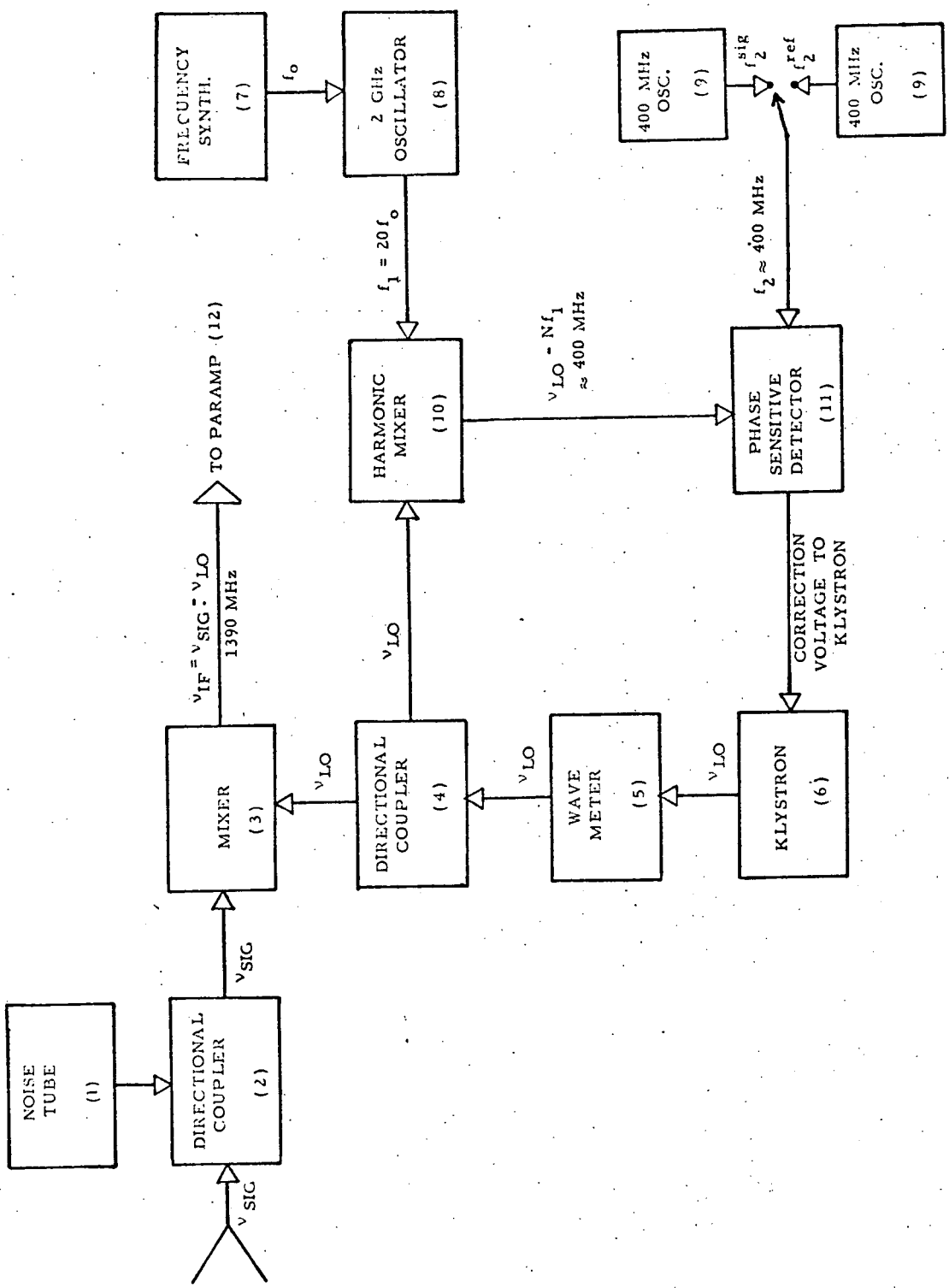
NOISE TUBE (1)
DIRECTIONAL COUPLER (2)
MIXER (3)
DIRECTIONAL COUPLER (4)
WAVE METER (5)
KLYSTRON (6)
FREQUENCY SYNTH. (7)
2 GHz OSCILLATOR (8)
400 MHz OSC. (9)
400 MHz OSC. (9)
HARMONIC MIXER (10)
PHASE SENSITIVE DETECTOR (11)
TO PARAMP (12)
ν_{SIG}
$\nu_{IF} = \nu_{SIG} - \nu_{LO}$
1390 MHz
ν_{LO}
f_o
$f_1 = 20 f_o$
$\nu_{LO} - N f_1 \approx 400$ MHz
$f_2 \approx 400$ MHz
f_2^{sig}
f_2^{ref}
CORRECTION VOLTAGE TO KLYSTRON

Figure 2

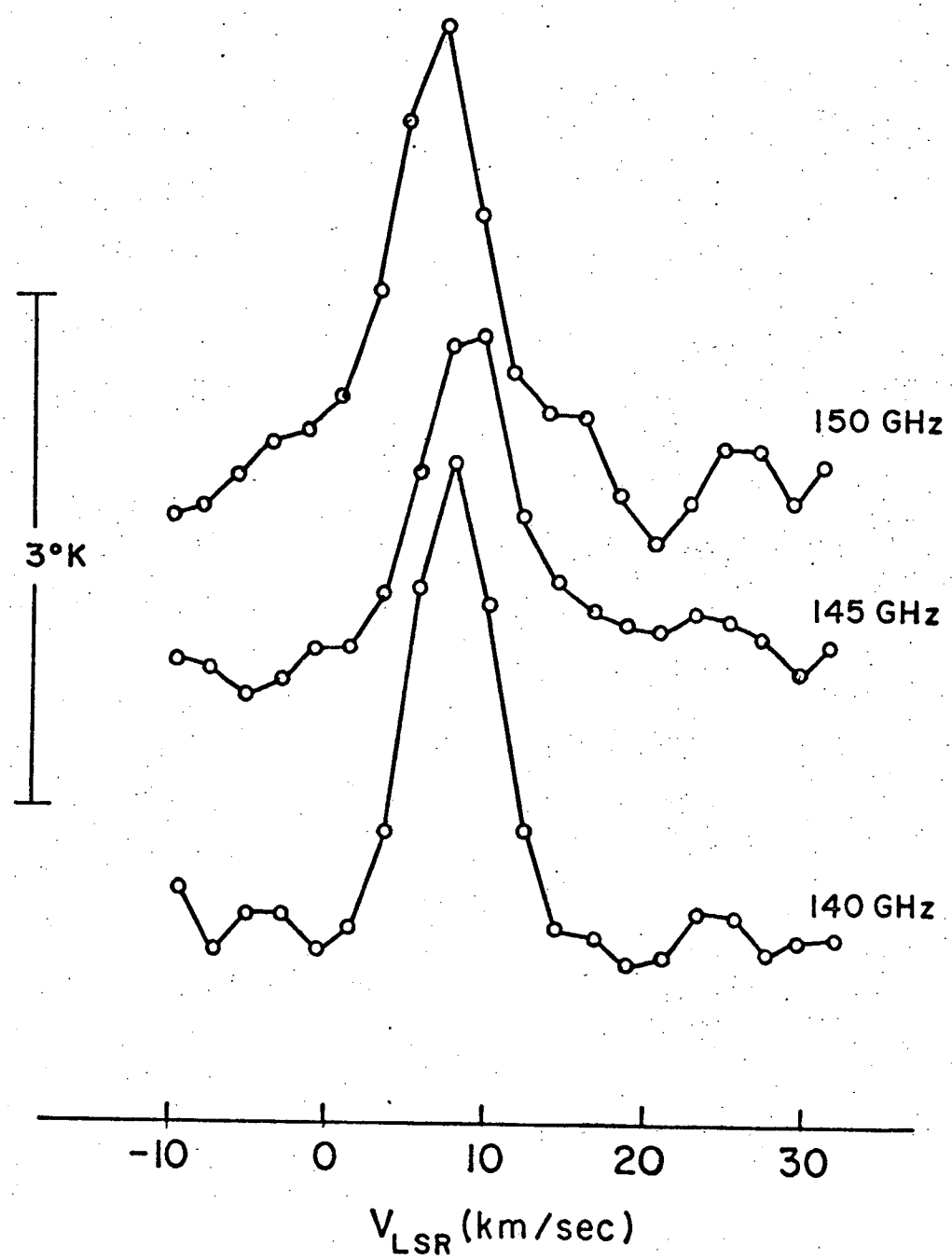

Figure 3

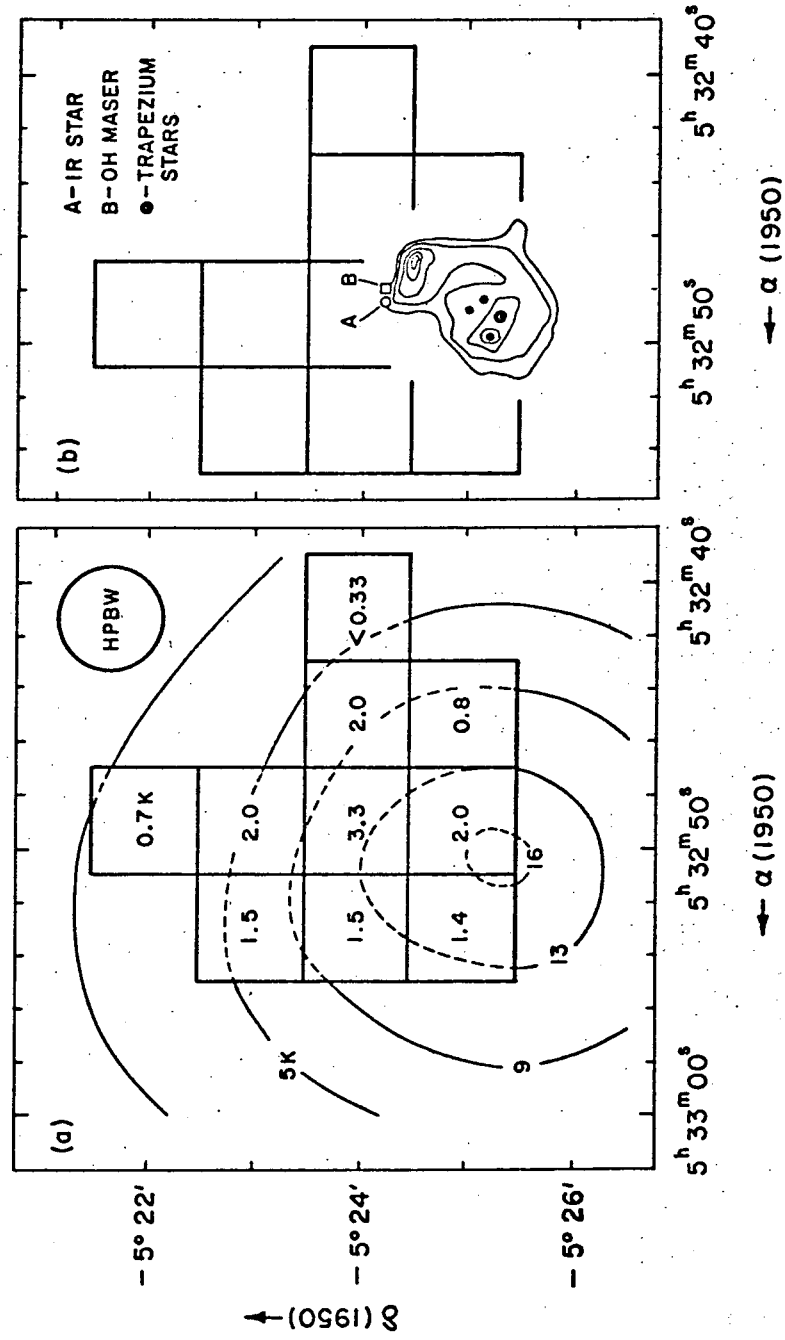
A-IR STAR
B-OH MASER
●-TRAPEZIUM STARS
(b)
A
B
5h 32m 40s
5h 32m 50s
α (1950)
(a)
HPBW
0.7 K
2.0
1.5
3.3
1.5
2.0
0.8
1.4
<0.33
16'
13
9
5K
5h 33m 00s
δ (1950)
-5° 22'
-5° 24'
-5° 26'

Figure 4

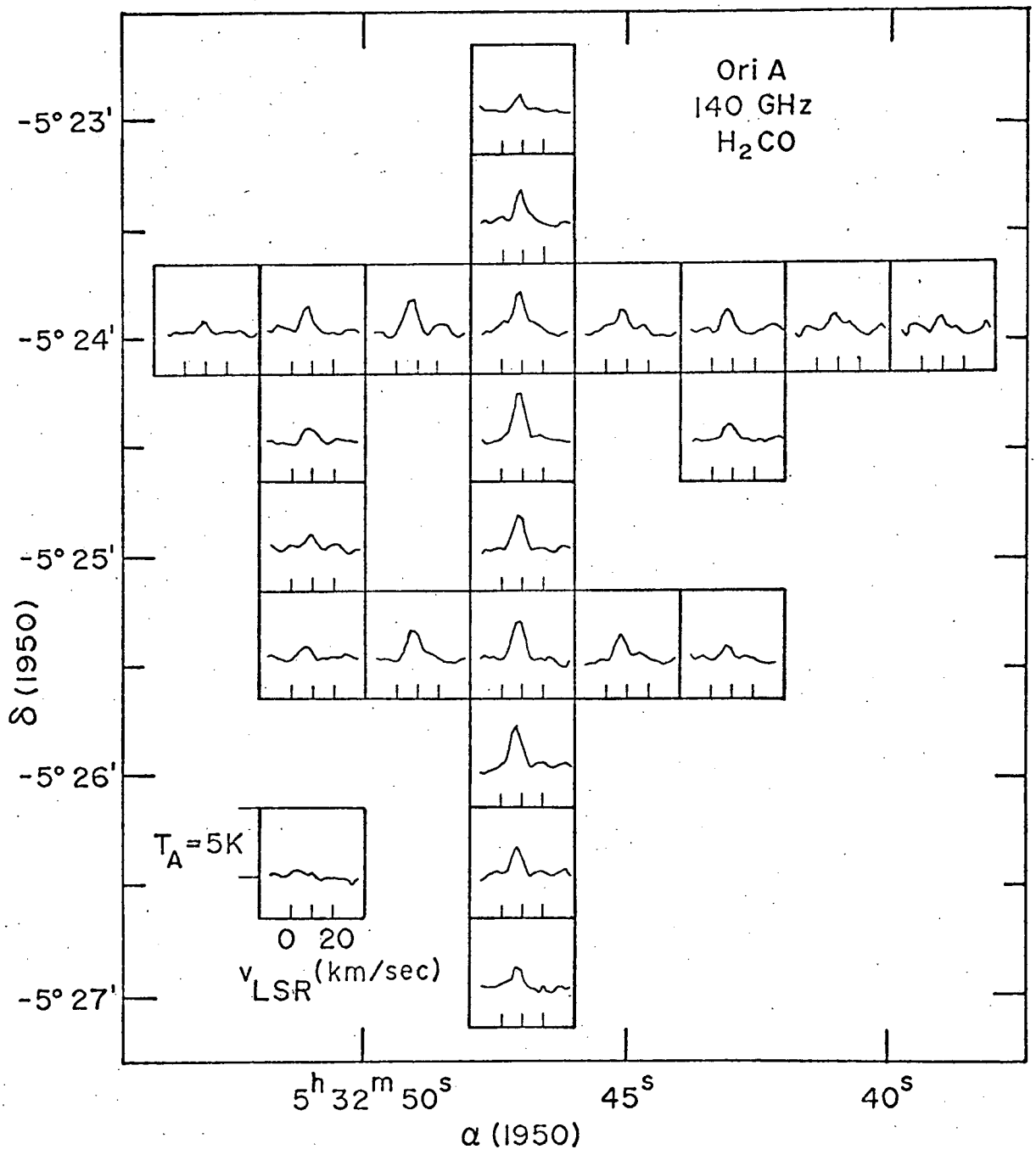
Ori A
140 GHz
H_2CO
-5° 23'
-5° 24'
-5° 25'
-5° 26'
-5° 27'
δ (1950)
T_A = 5K
0 20
v_{LSR} (km/sec)
$5^h 32^m 50^s$
45^s
40^s
α (1950)

Figure 5

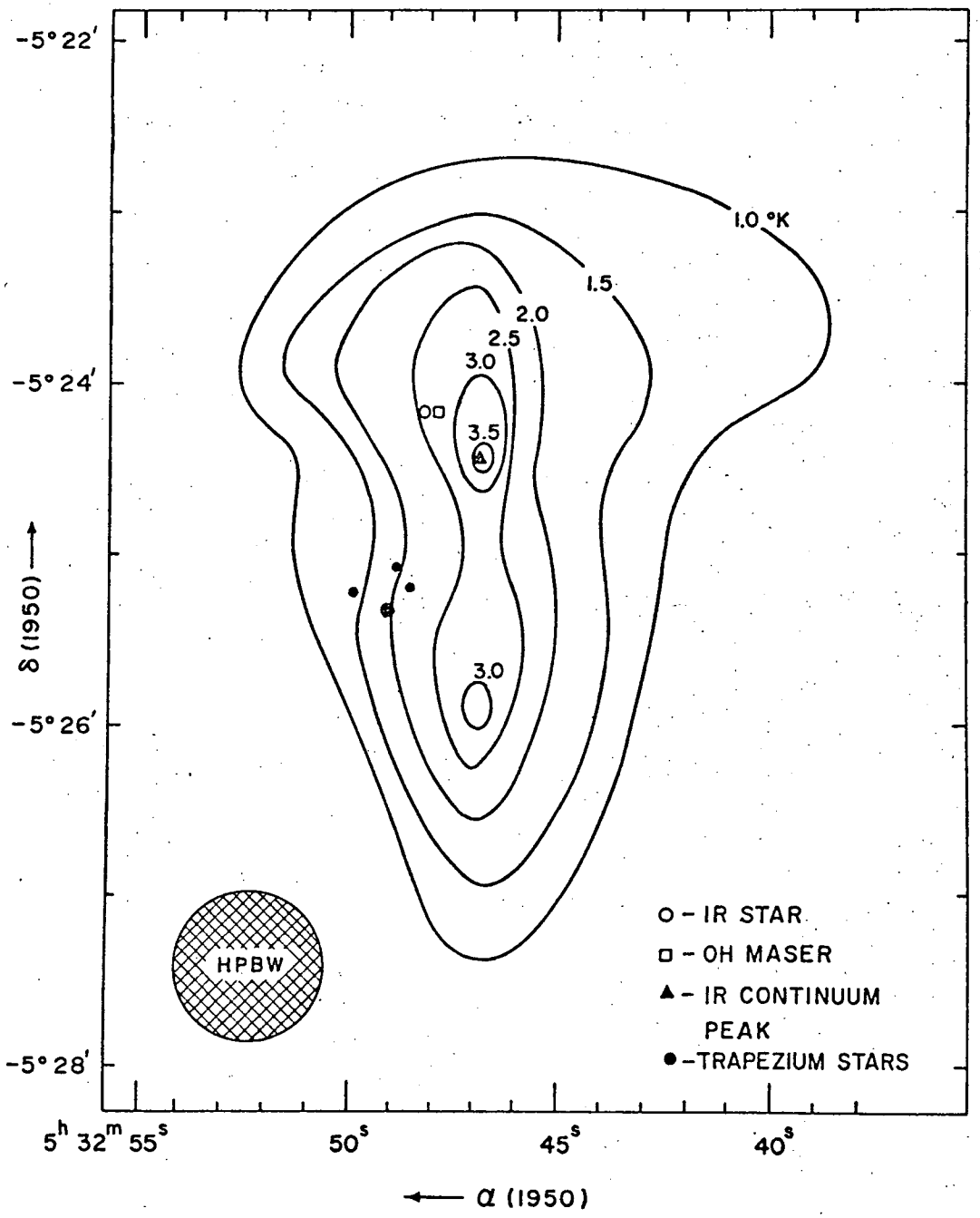
-5°22'
-5°24'
-5°26'
-5°28'
δ (1950)
1.0 °K
1.5
2.0
2.5
3.0
3.5
3.0
HPBW
O - IR STAR
□ - OH MASER
▲ - IR CONTINUUM PEAK
● - TRAPEZIUM STARS
5h 32m 55s
50s
45s
40s
α (1950)

Figure 6

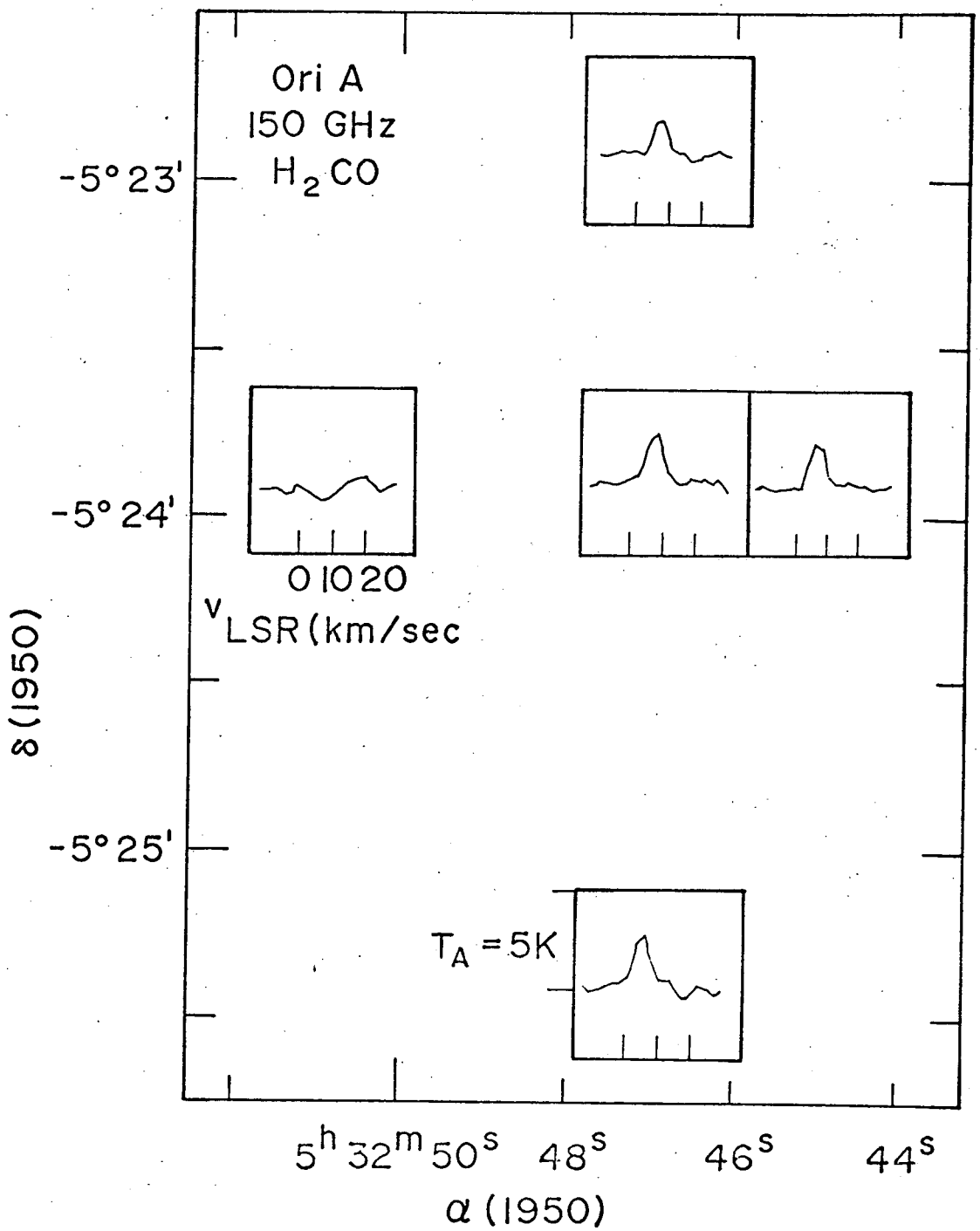
Ori A
150 GHz
H_2CO
-5° 23'
-5° 24'
-5° 25'
0 10 20
v_{LSR} (km/sec
T_A = 5K
δ (1950)
$5^h 32^m 50^s$
48^s
46^s
44^s
α (1950)

Figure 7

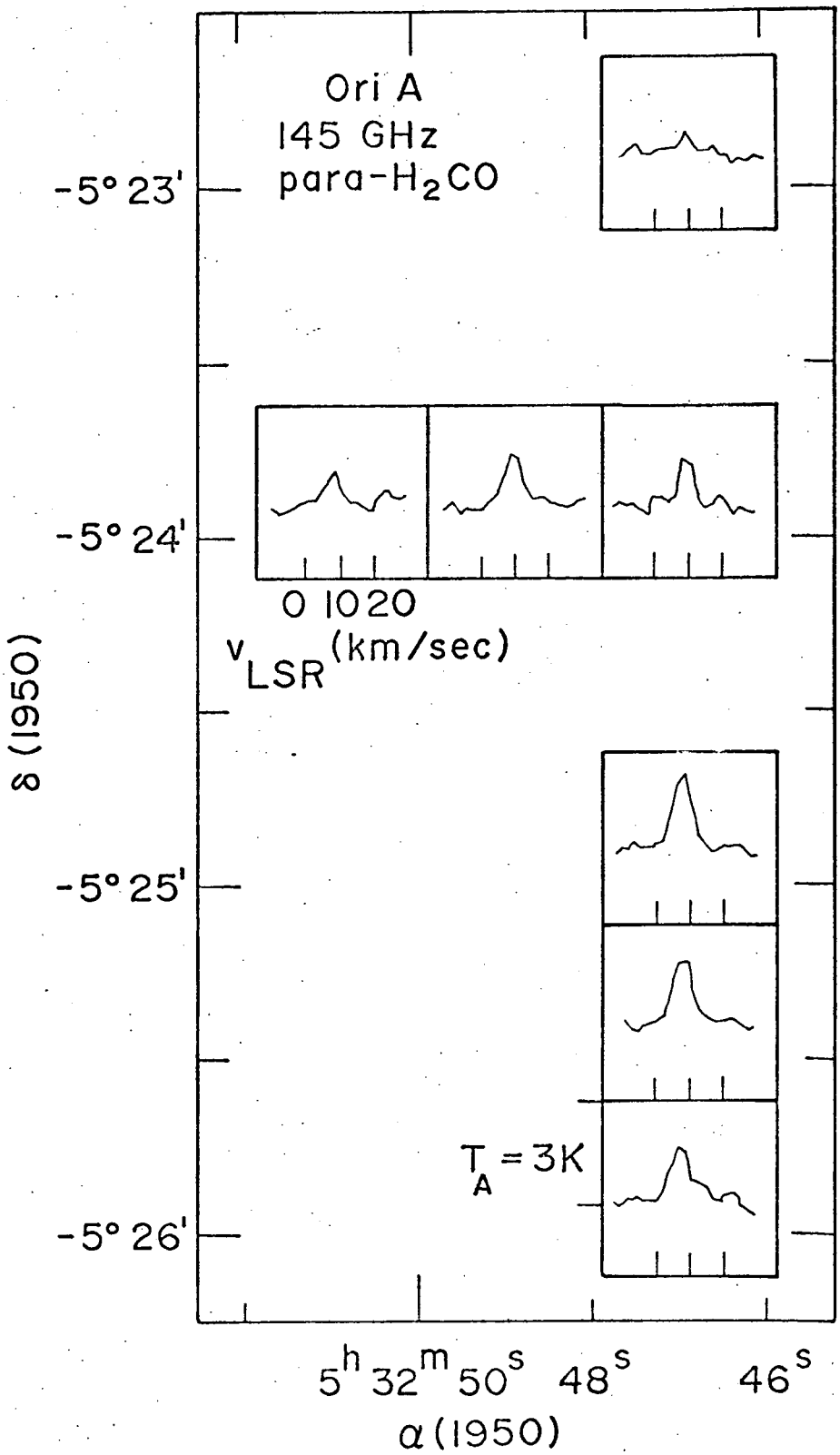
Ori A
145 GHz
para-H_2CO
-5° 23'
-5° 24'
-5° 25'
-5° 26'
0 10 20
v_{LSR} (km/sec)
T_A = 3K
δ (1950)
$5^h\,32^m\,50^s$
48^s
46^s
α (1950)

Figure 8

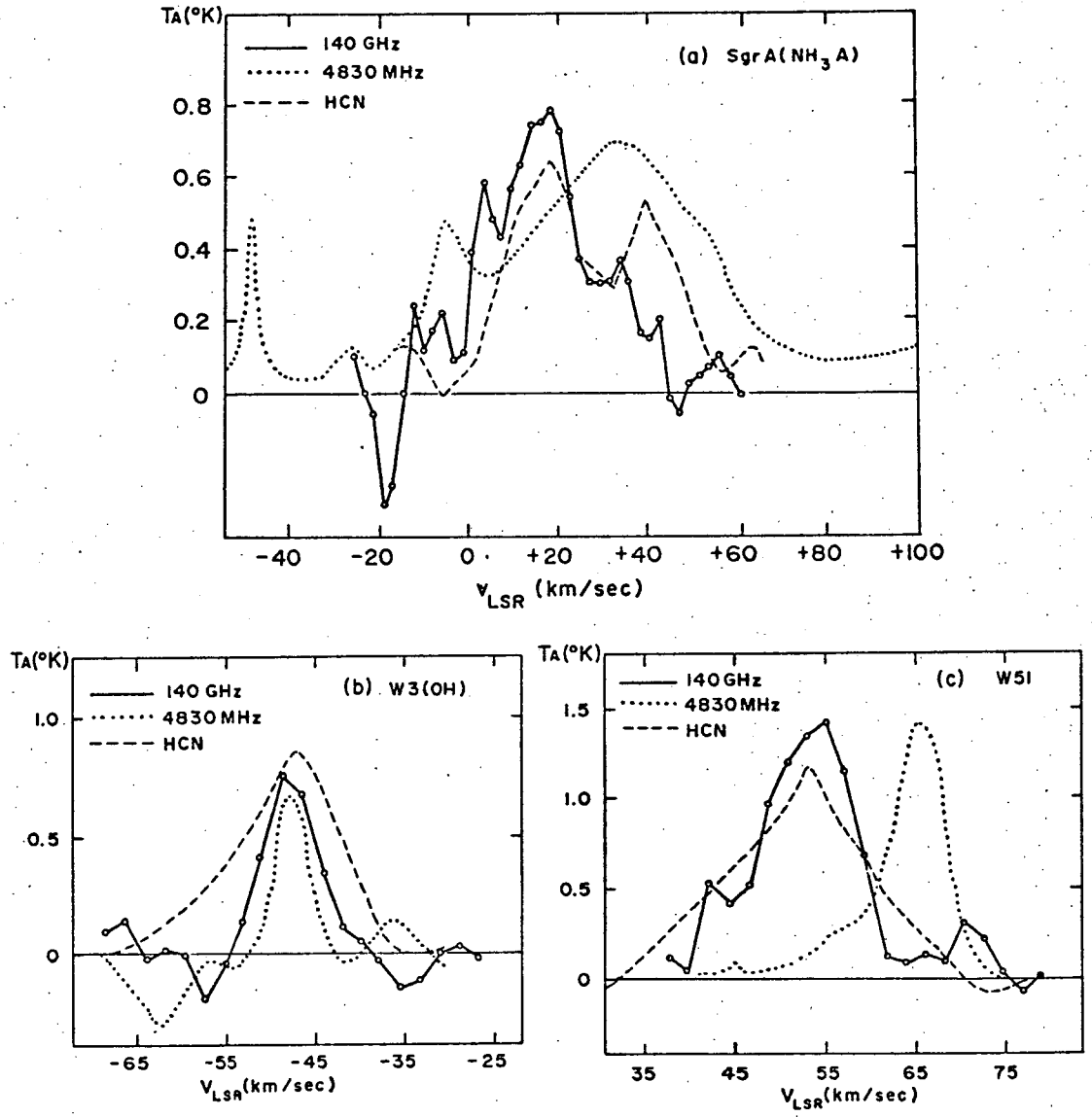
TA(°K)
140 GHz
4830 MHz
HCN
(a) SgrA(NH3 A)
0.8
0.6
0.4
0.2
0
-40
-20
0
+20
+40
+60
+80
+100
VLSR (km/sec)
TA(°K)
140 GHz
4830 MHz
HCN
(b) W3(OH)
1.0
0.5
0
-65
-55
-45
-35
-25
VLSR(km/sec)
TA(°K)
140 GHz
4830 MHz
HCN
(c) W51
1.5
1.0
0.5
0
35
45
55
65
75
VLSR(km/sec)

Figure 9

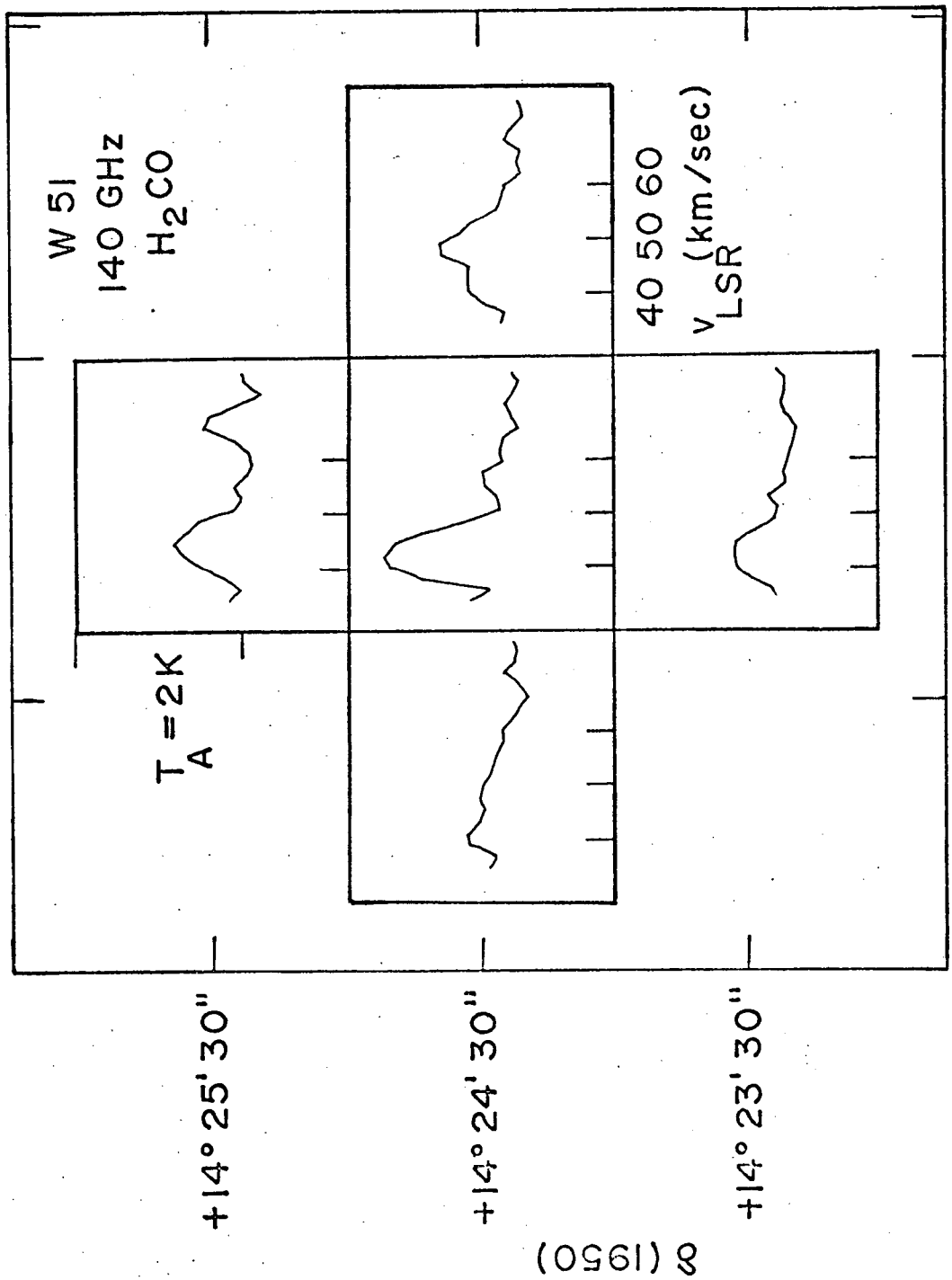
W 51
140 GHz
H_2CO
T_A = 2K
40 50 60
v_{LSR} (km/sec)
+14° 25' 30"
+14° 24' 30"
+14° 23' 30"
δ (1950)
19h 21m 30s
25
α (1950)

Figure 10

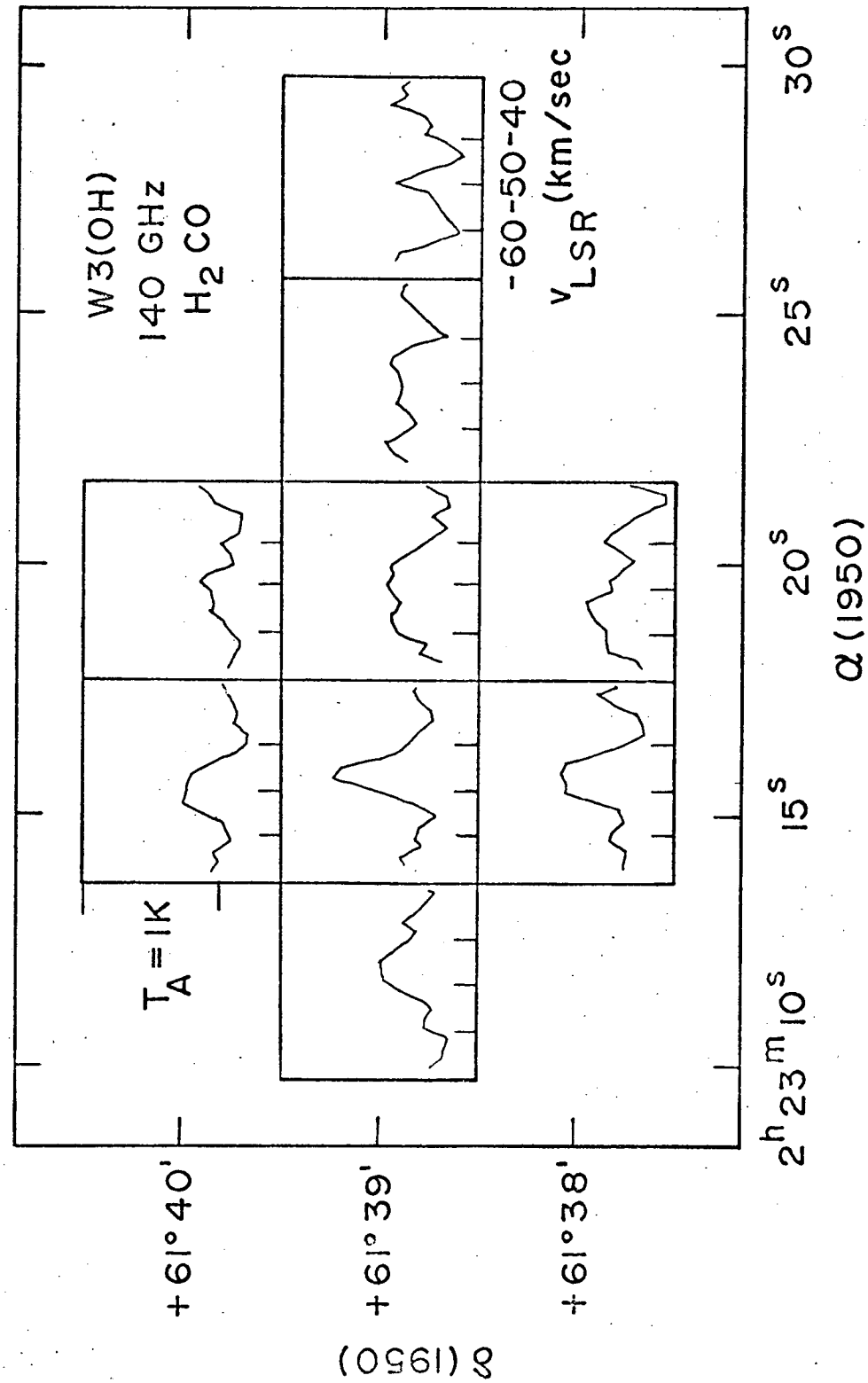
W3(OH)
140 GHz
H_2CO
T_A = 1K
-60-50-40
v_{LSR} (km/sec
+61°40'
+61°39'
+61°38'
$2^h23^m10^s$
15s
20s
25s
30s
α (1950)
δ (1950)

Figure 11

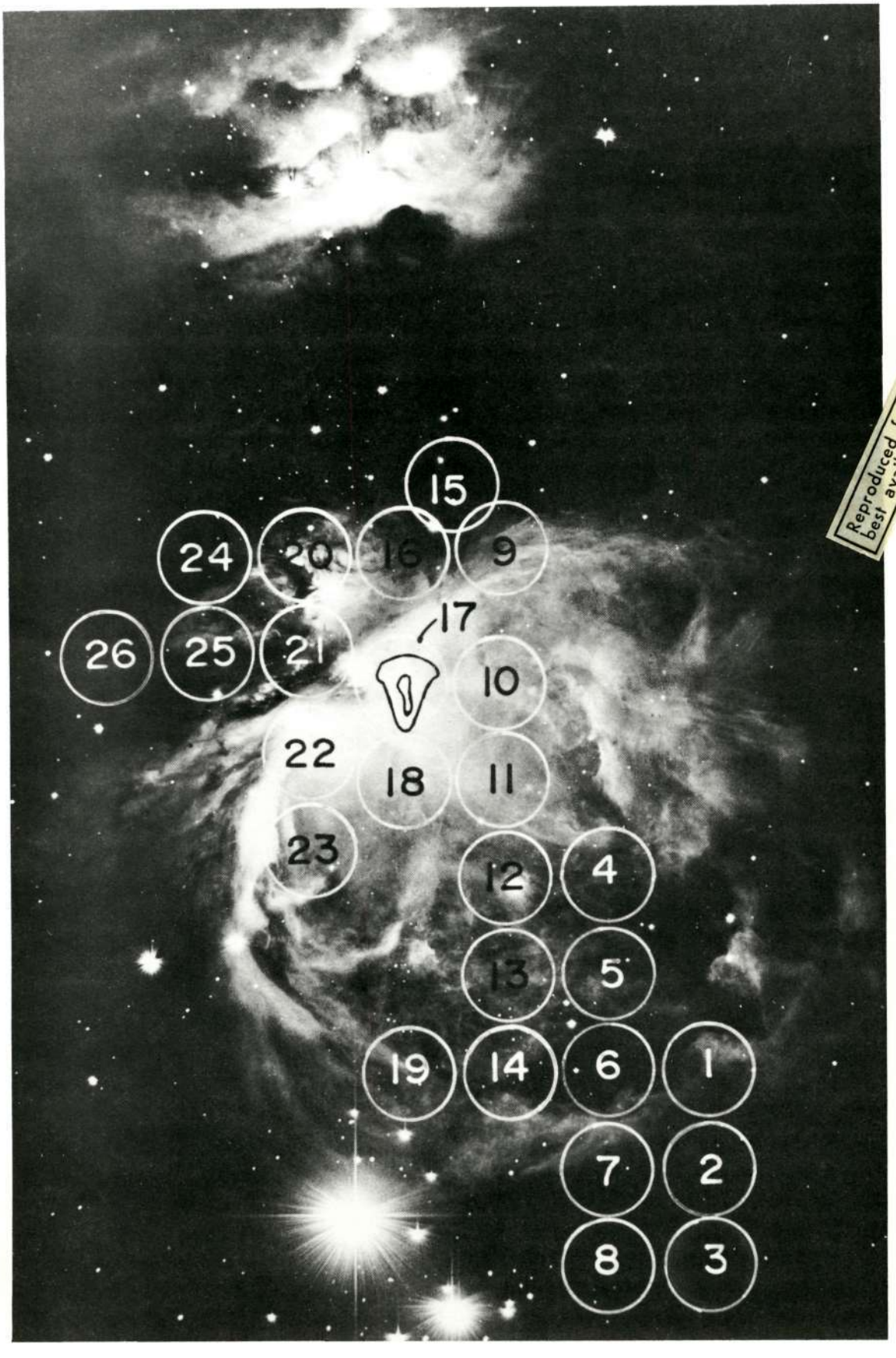

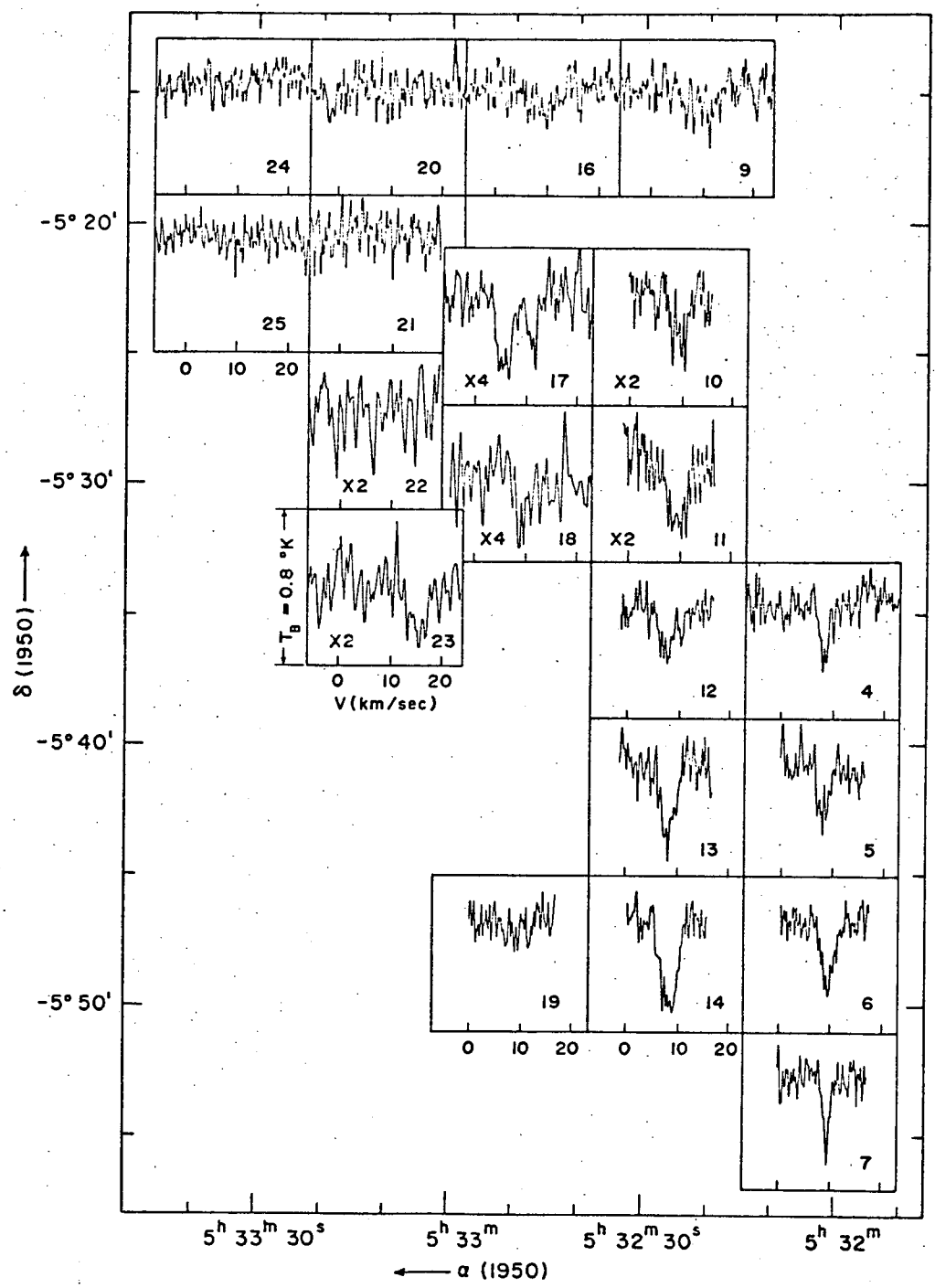
-5° 20'
-5° 30'
-5° 40'
-5° 50'
δ (1950)
24
20
16
9
25
21
X4
17
X2
10
X2
22
X4
18
X2
11
X2
23
12
4
13
5
19
14
6
7
0 10 20
T_B = 0.8 °K
V (km/sec)
$5^h 33^m 30^s$
$5^h 33^m$
$5^h 32^m 30^s$
$5^h 32^m$
α (1950)

Figure 13

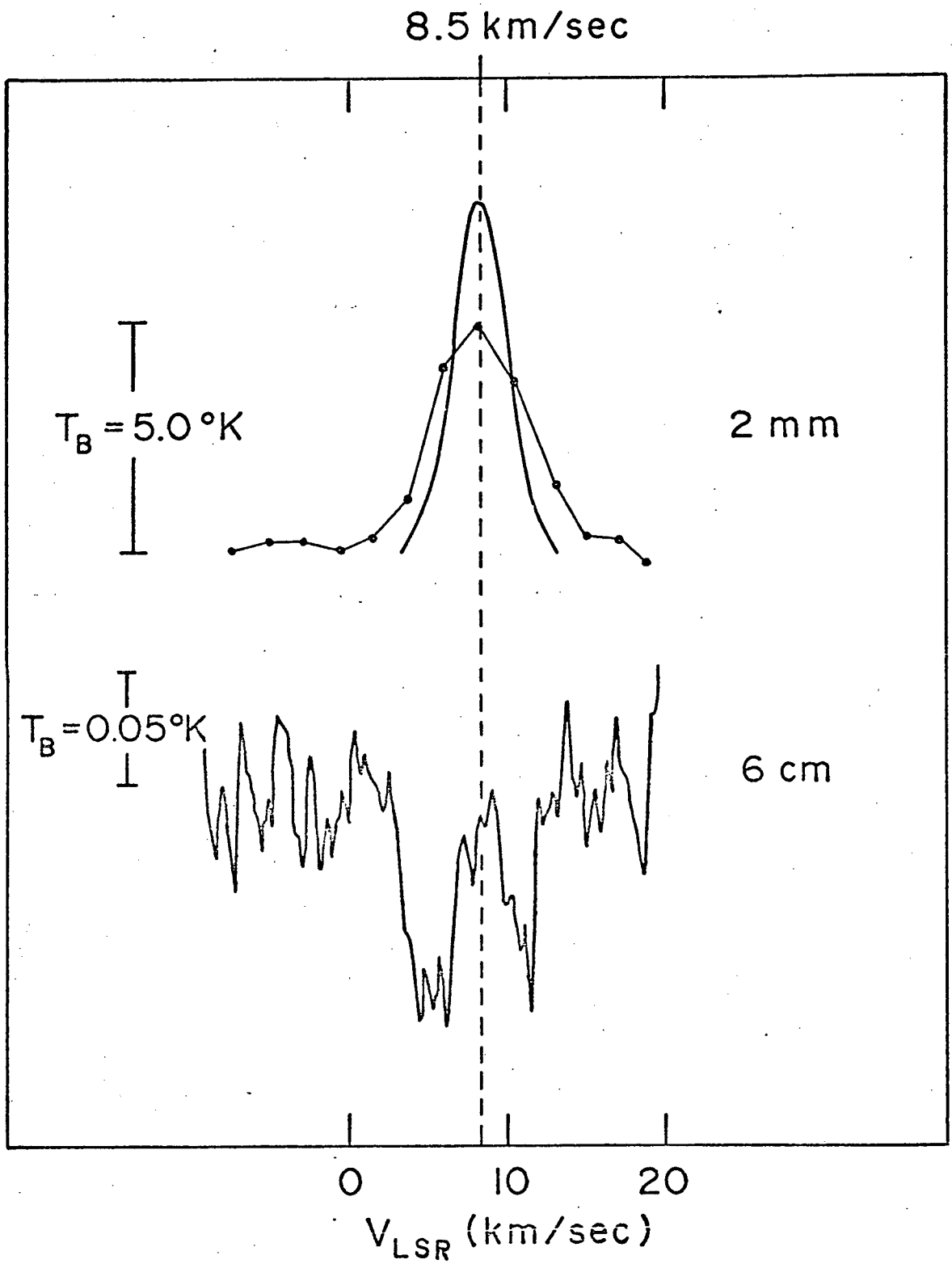

Figure 14

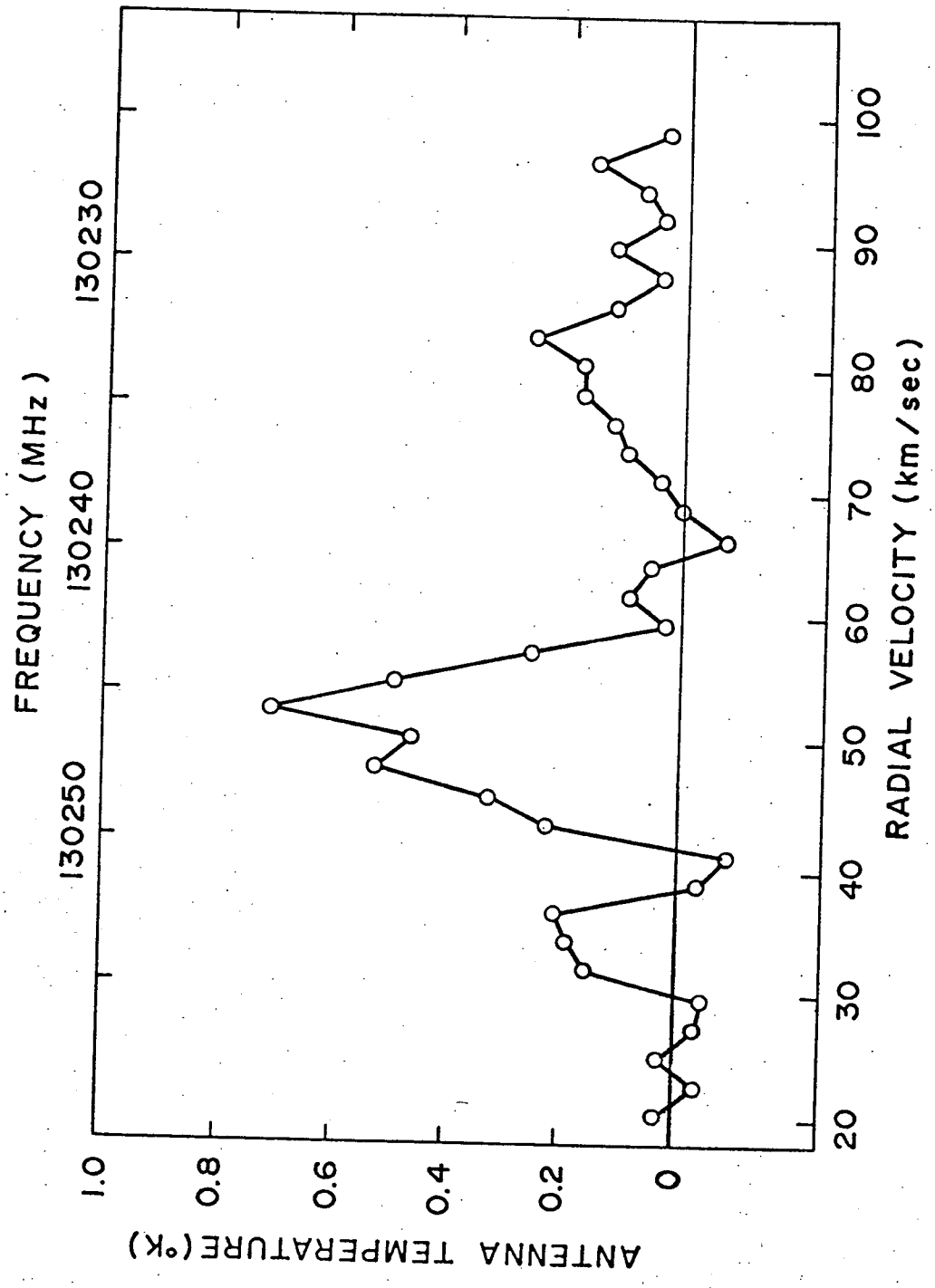
FREQUENCY (MHz)
130230
130240
130250
RADIAL VELOCITY (km/sec)
20
30
40
50
60
70
80
90
100
ANTENNA TEMPERATURE (°K)
0
0.2
0.4
0.6
0.8
1.0

Figure 15